The Abdus Salam
International Centre
for Theoretical Physics

United Nations Educational, Scientific and Cultural Organization

IAEA International Atomic Energy Agency

2464-17

Earthquake Tectonics and Hazards on the Continents

17 - 28 June 2013

Recognizing and characterizing blind thrust faults and earthquakes

R. Walker
University of Oxford
UK

Recognising thrust faults and earthquakes: examples from Asia

The Zagros, Iran (NASA)

Continental shortening

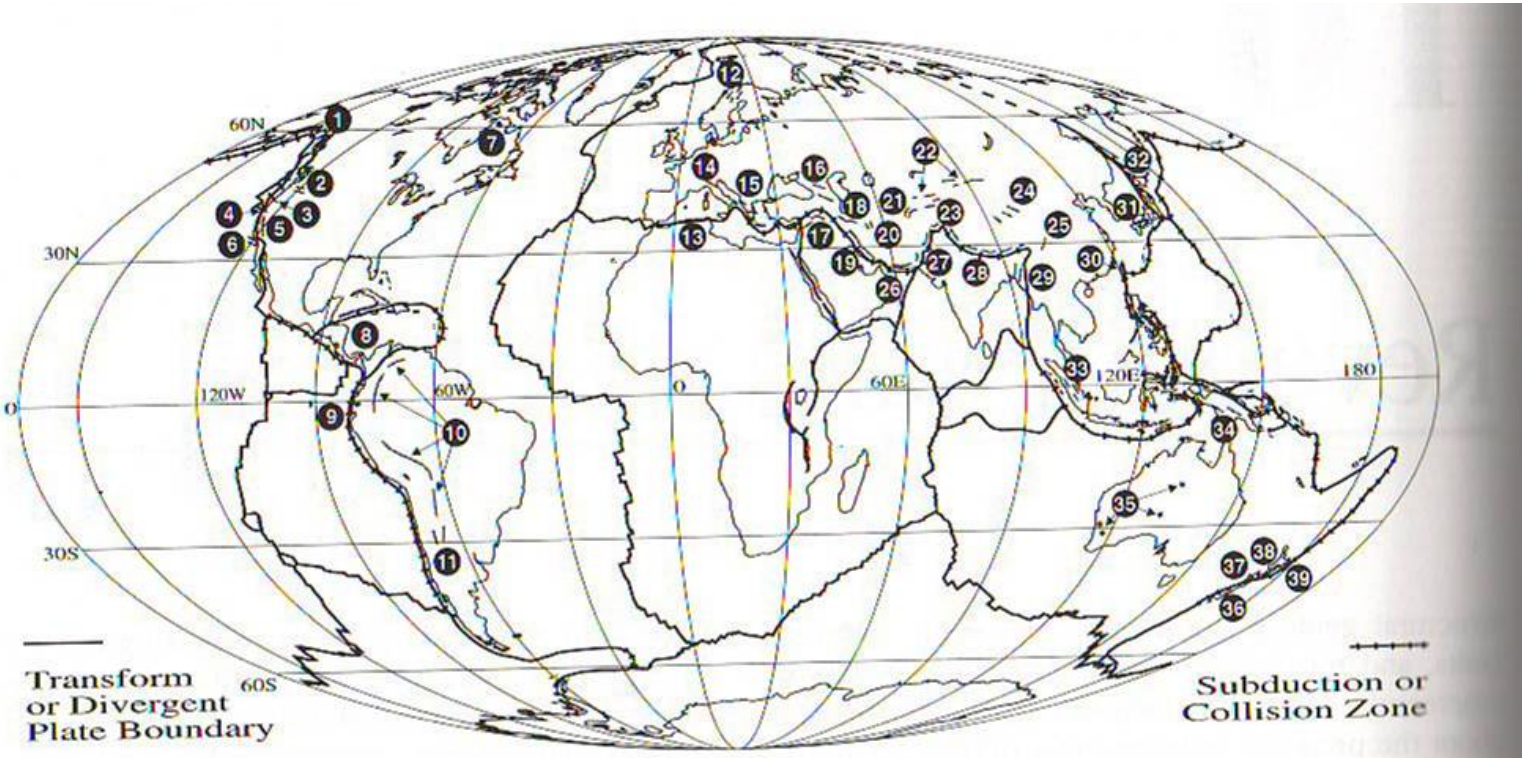

Figure 10–1. Locations of major active onshore reverse fault and fold systems. 1. Pamplona-Kayak Island zone, Alaska (largely offshore); 2. Yakima fold belt, Washington; 3. Cape Arago, Oregon (partly offshore); 4. northern California coast (partly offshore); 5. Coast Ranges, California; 6. western Transverse Ranges, California (partly offshore); 7. Ungava, Canada; 8. North Panama deformed belt (largely offshore); 9. Inter-Andean depression, Ecuador; 10. Subandean Cordillera; 11. Pampean Andes, Argentina; 12. northern Scandinavia; 13. Tellian Atlas, north Africa; 14. southern margin of Po Plain, Italy; 15. Epirus, Greece; 16. Greater and Lesser Caucasus; 17. Bitlis foldthrust belt and Palmyride fold belt; 18. Alborz Mountains, Iran; 19. Zagros Mountains; 20. Khorassan, Iran; 21. Tajikistan; 22. northern range front of Tianshan; 23. southern range front of Tianshan, China; 24. Qilian Shan-Qaidam basin, China; 25. Lungmen Shan-Min Shan, China; 26. Makran (partly offshore); 27. Kirthar and Sulaiman Ranges, Pakistan; 28. Himalayan frontal thrust; 29. Arakan fold belt, Burma; 30. Taiwan coastal plain; 31. Kinki Triangle, Japan; 32. Niigata fold belt, northern Japan (partly offshore); 33. central Sumatra; 34. Papua New Guinea; 35. Australia; 36. Central Otago, New Zealand; 37. northwest Nelson, New Zealand; 38. Wanganui folds, New Zealand; 39, East Coast Fold Belt, New Zealand (partly offshore)

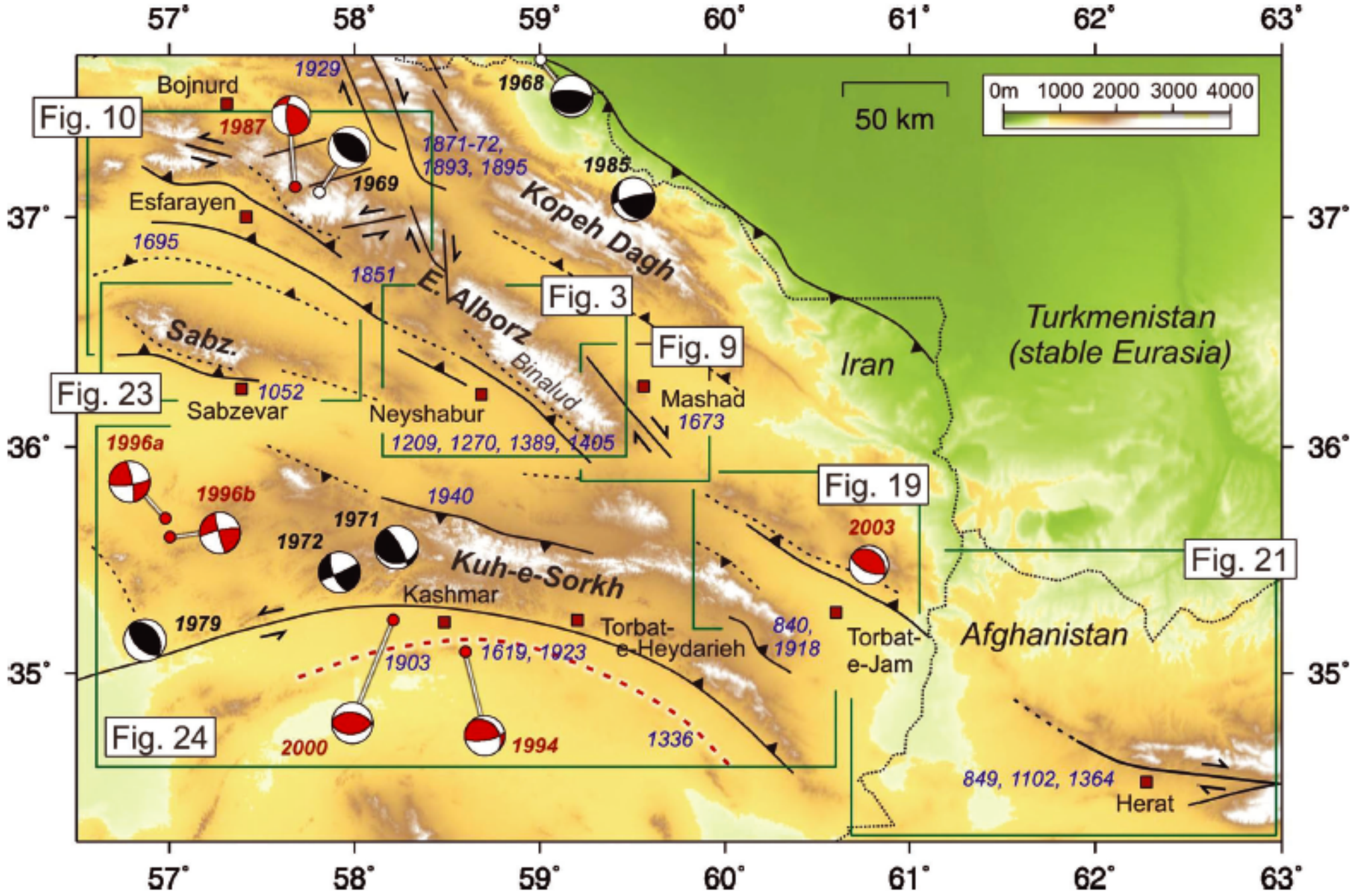

Hollingsworth et al. 2010

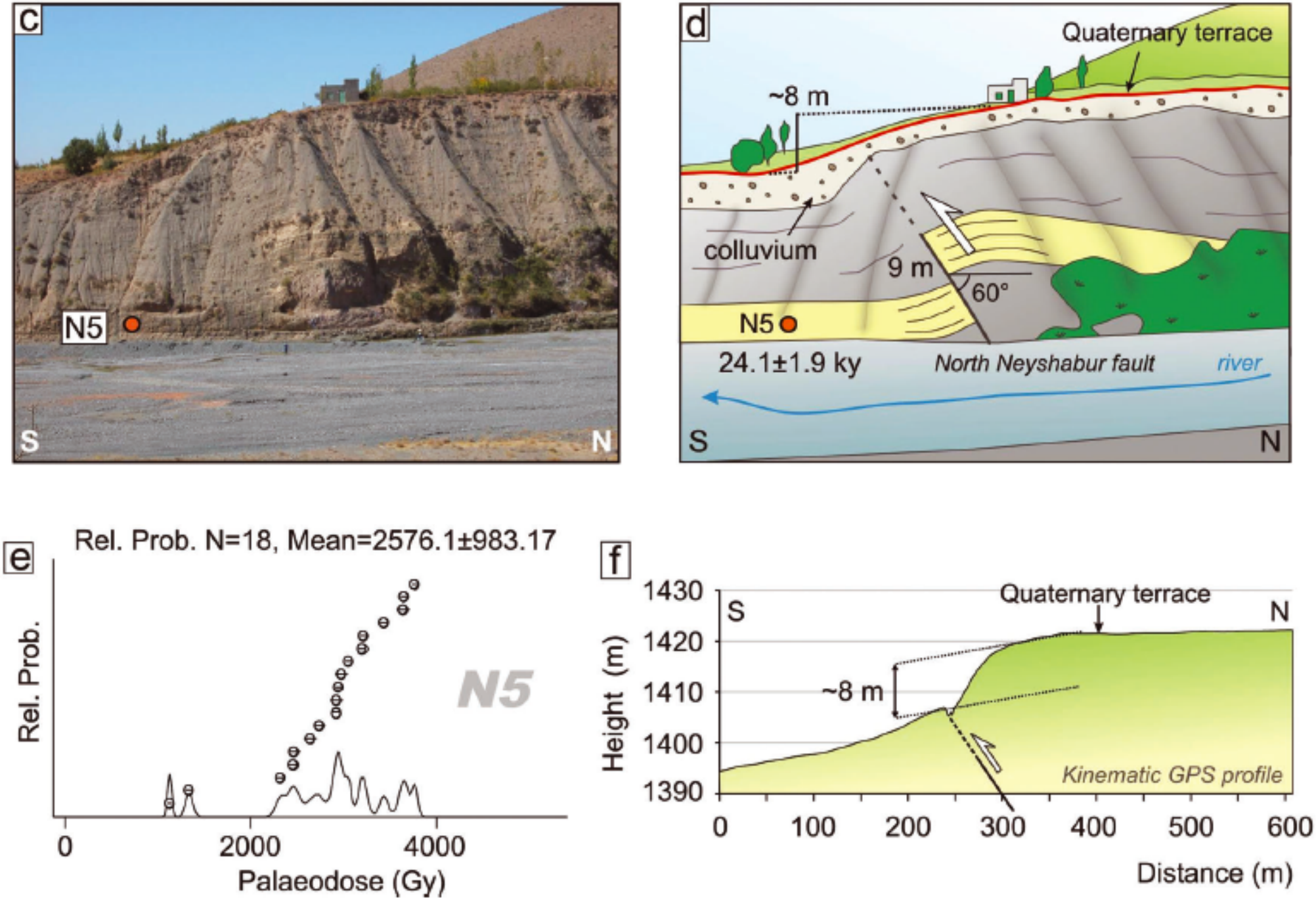
c
N5
S
N
d
Quaternary terrace
~8 m
colluvium
9 m
60°
N5
24.1±1.9 ky
North Neyshabur fault
river
S
N
e
Rel. Prob. N=18, Mean=2576.1±983.17
Rel. Prob.
N5
0
2000
4000
Palaeodose (Gy)
f
1430
1420
1410
1400
1390
Height (m)
S
N
Quaternary terrace
~8 m
Kinematic GPS profile
0
100
200
300
400
500
600
Distance (m)

An example of an active zone of shortening – the Tien Shan

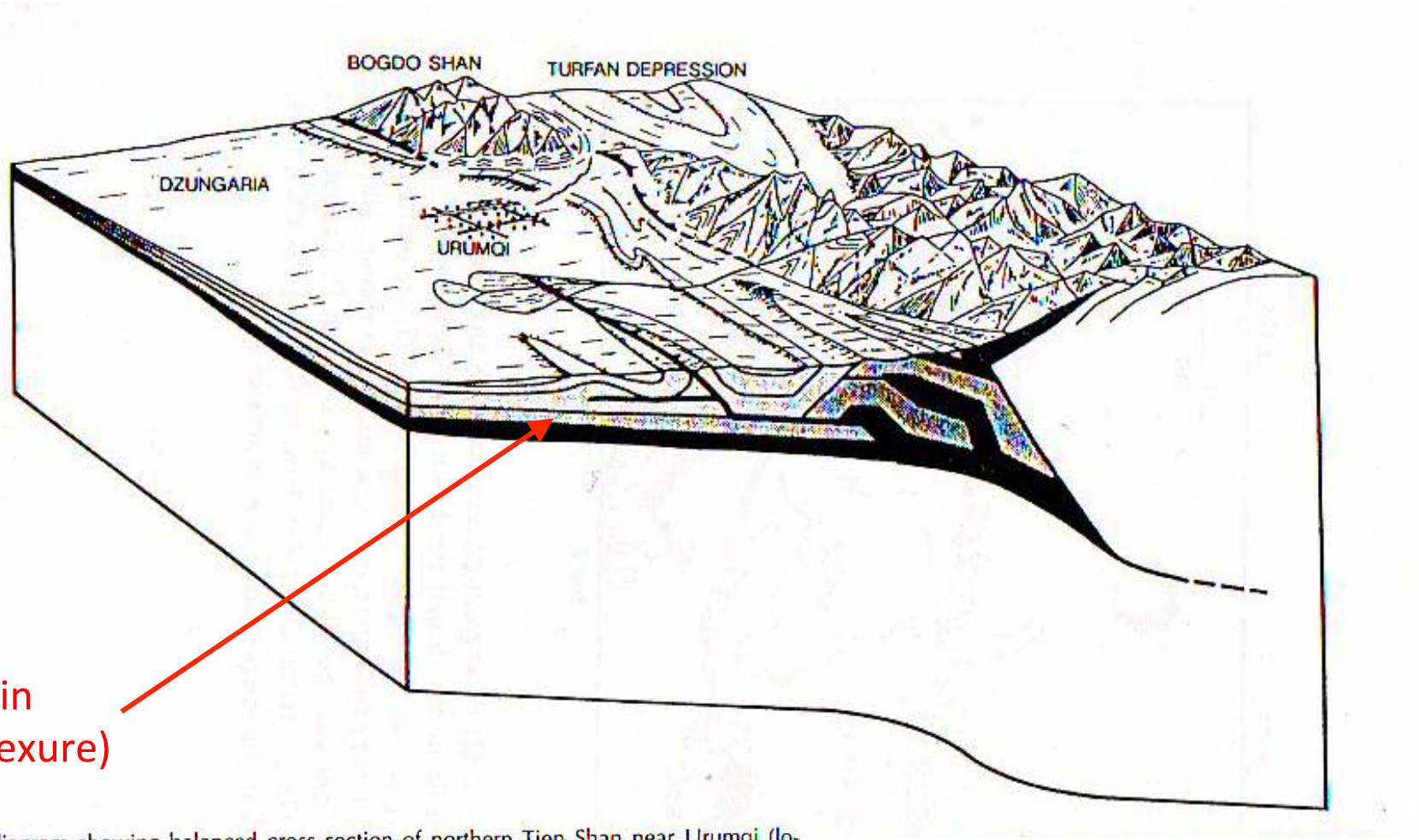

Figure 10–24. Block diagram showing balanced cross section of northern Tien Shan near Urumqi (located on Fig. 10–23). Active anticlines are interpreted as surface expression of thrust faults that ramp upward toward the surface and migrate toward the basin with time. The Tien Shan itself rides upward on a ramp that involves the entire brittle crust. Sedimentary rocks are Permian and younger, with the lightest pattern representing Upper Cretaceous and younger strata. After Avouac et al. (1993).

As faulting migrates into the foreland it incorporates old foreland basin sediments

Thrusting and folding …

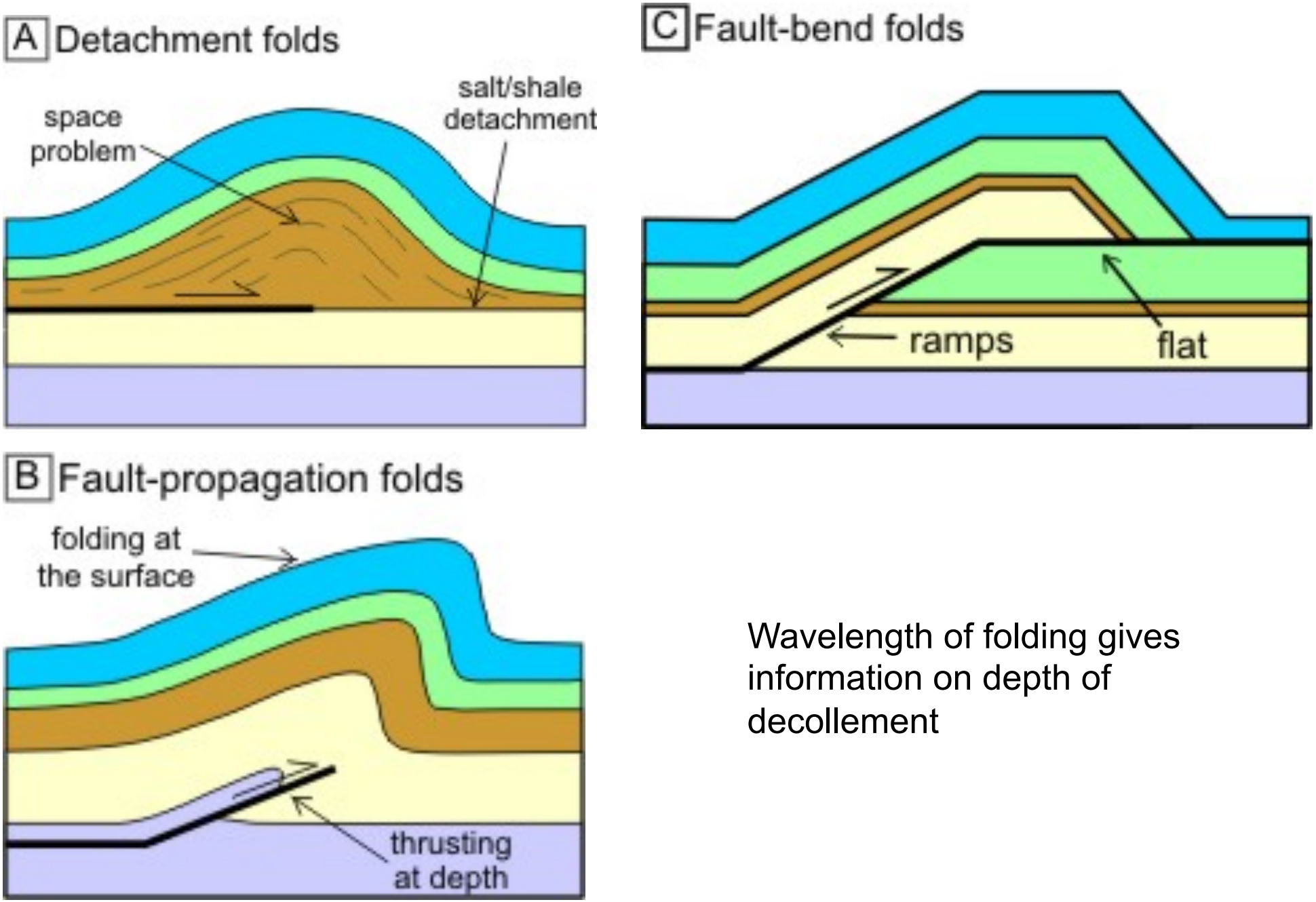

Wavelength of folding gives information on depth of decollement

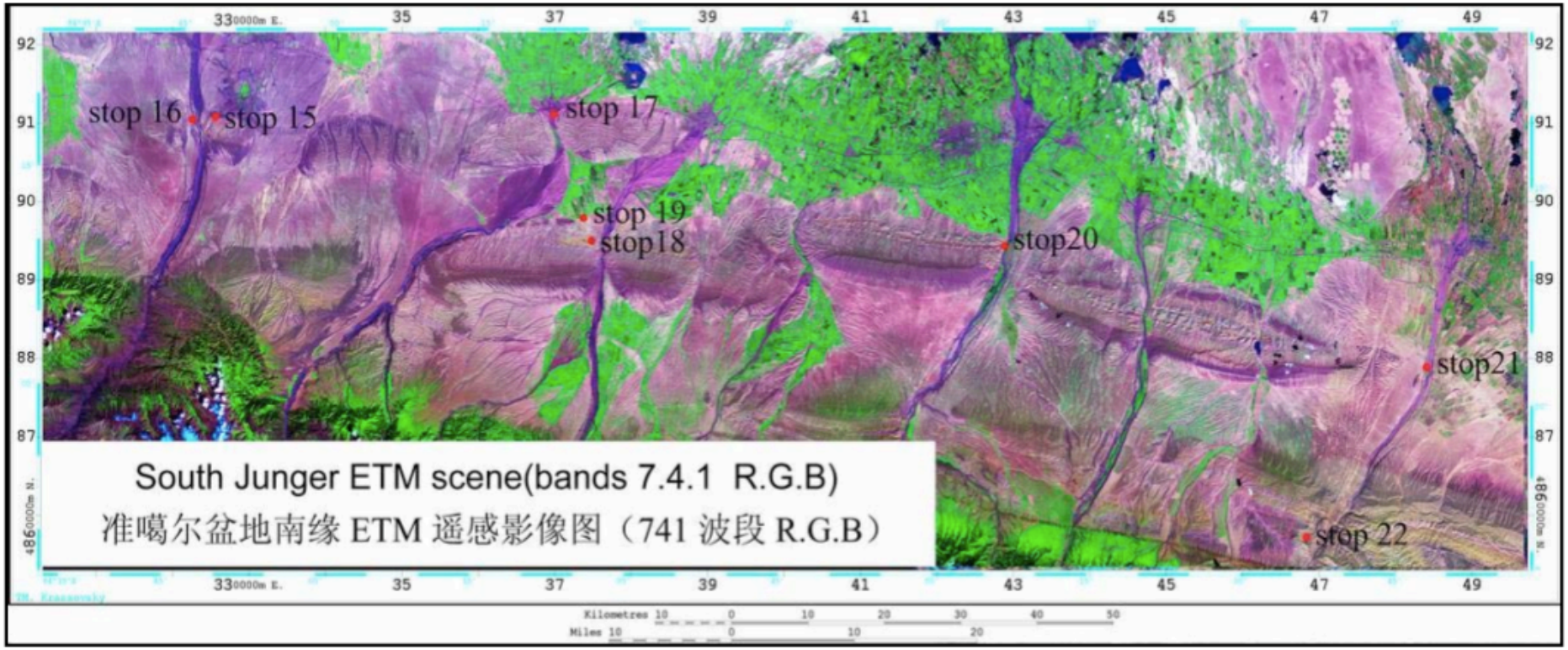
stop 16
stop 15
stop 17
stop 19
stop18
stop20
stop21
stop 22
South Junger ETM scene(bands 7.4.1 R.G.B)
准噶尔盆地南缘 ETM 遥感影像图（741 波段 R.G.B）

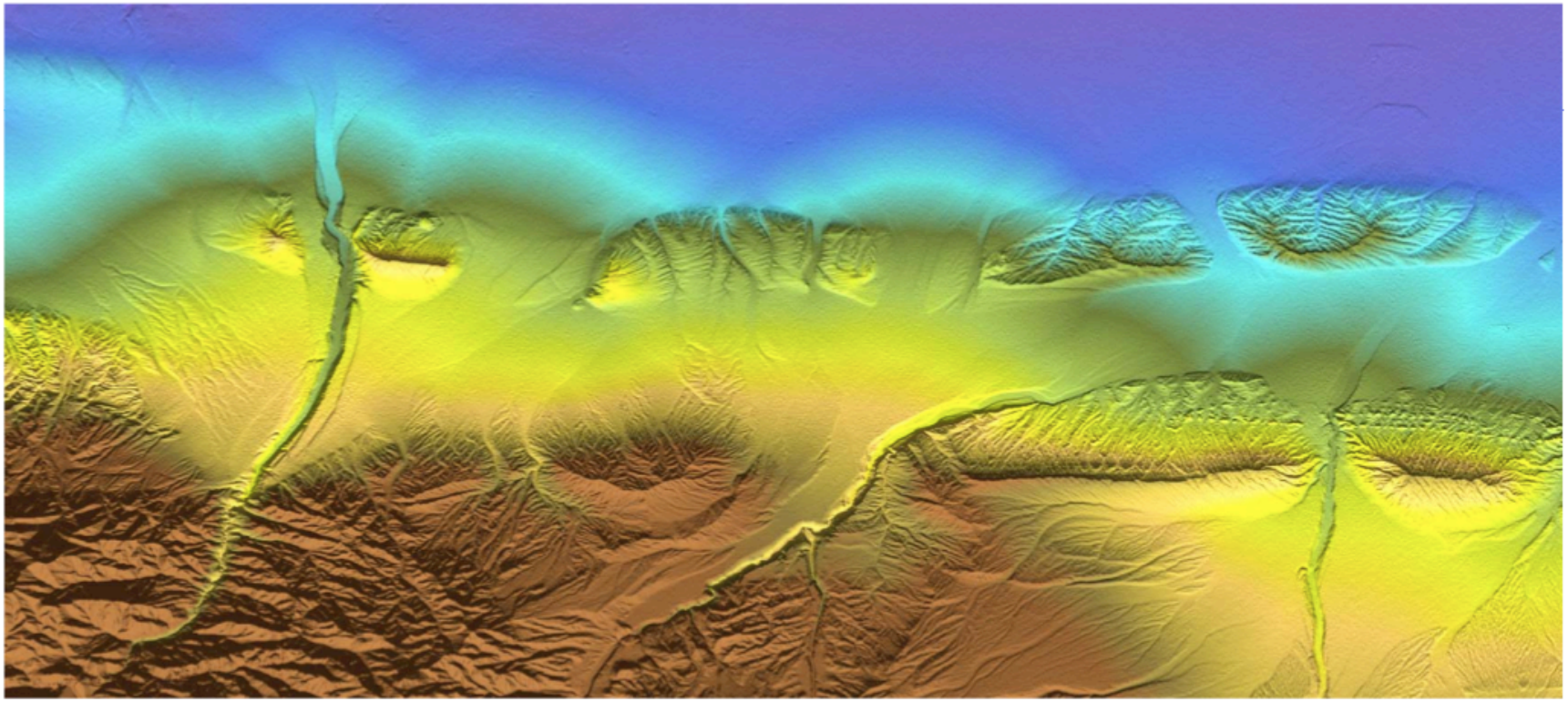

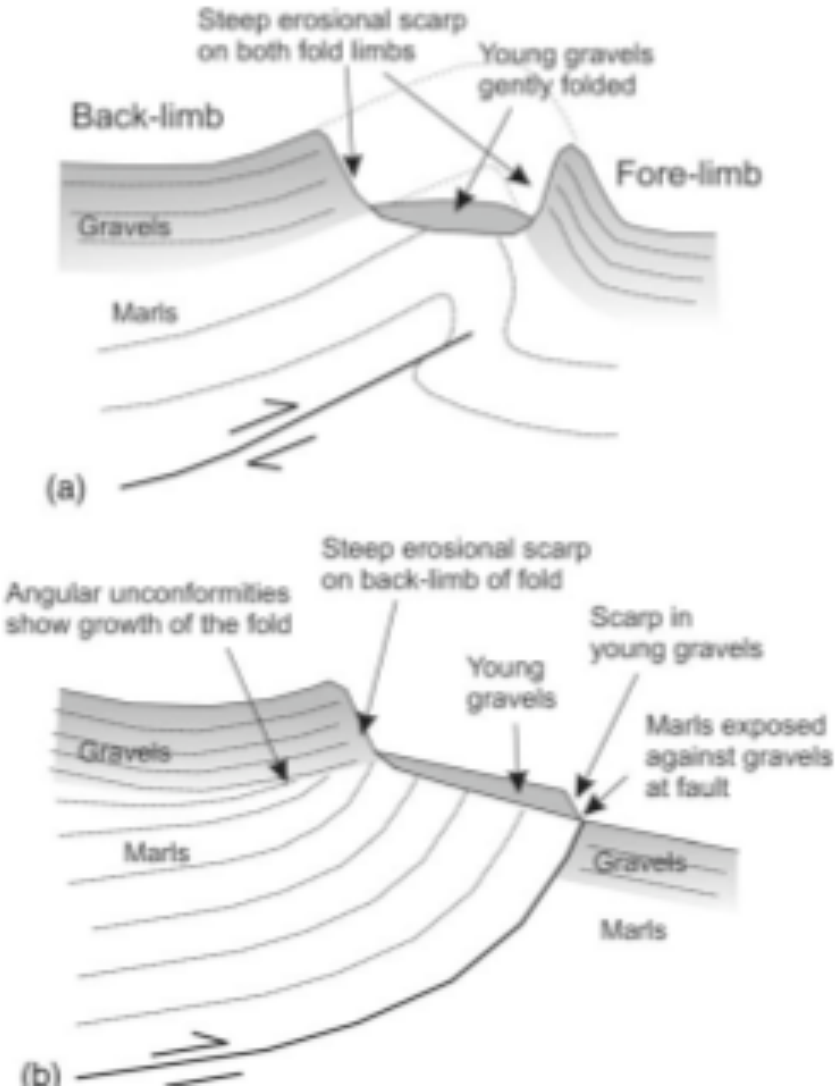

Walker, 2006

Shahdad fold-thrust belt (eastern Iran)

Fault Growth in Central Otago, New Zealand

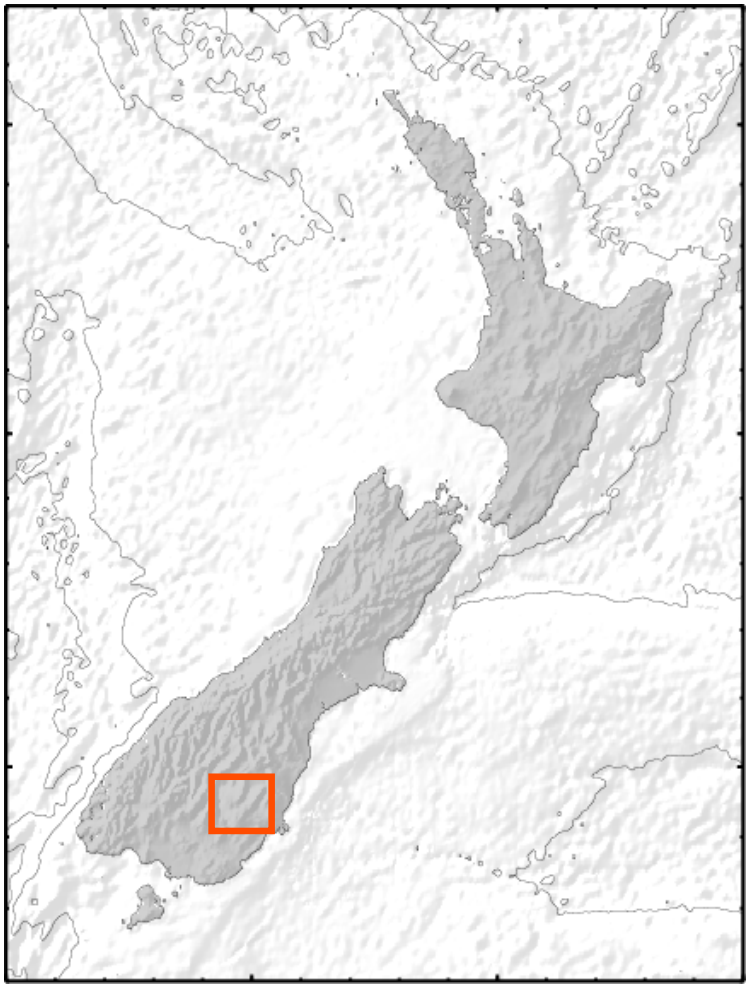

Main geomorphological feature of Central Otago is peneplain surface that is flat except where warped into a series of parallel ridges and valleys by folds and reverse thrusts trending NE-SW. These active structures accommodate a few mm/yr of the 35-40mm/yr oblique convergence between the Australian and Pacific plates, most of which is taken up across the Alpine Fault and Southern Alps.

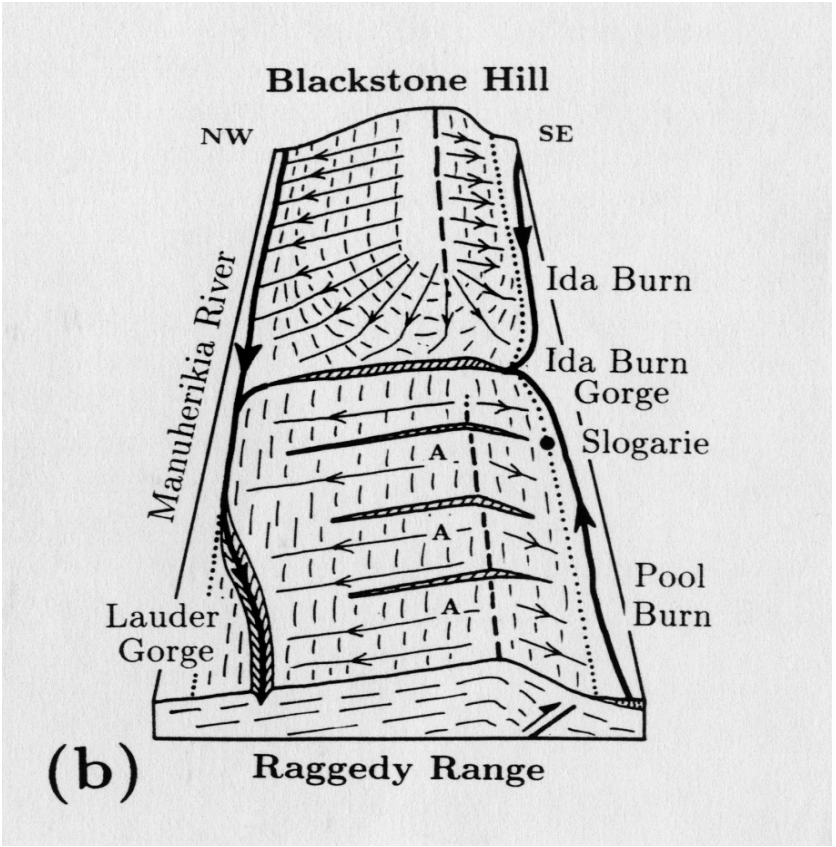

Jackson et.al. 1996

Lateral fold growth

Note: Wind-gaps are found in areas of normal faulting too!

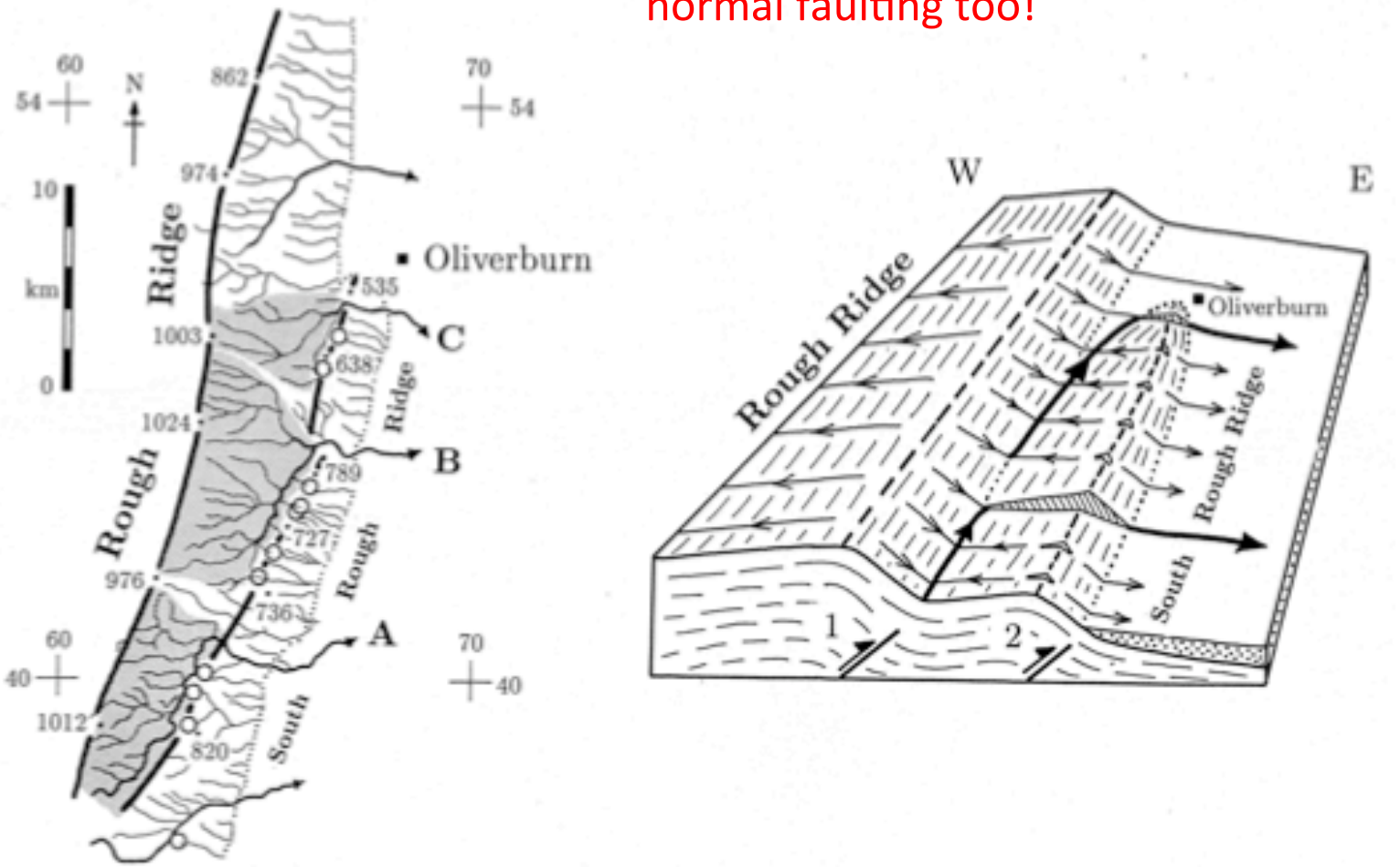

Fig. 57. (a) Drainage map of the region between Rough Ridge and South Rough Ridge near Oliverburn (Fig. 56). Thick solid lines are drainage divides. The catchments for streams A, B and C are shaded. Wind gaps are marked by open circles and spot heights are in m. (b) Cartoon to illustrate the structure and drainage in (a). Note the dry wind gaps in the frontal ridge. The gathering of the major streams into asymmetric catchments that cross South Rough Ridge suggests that the fault underlying it (2) is later than the one forming Rough Ridge (1) and also propagating north. From Jackson *et al.* [1996].

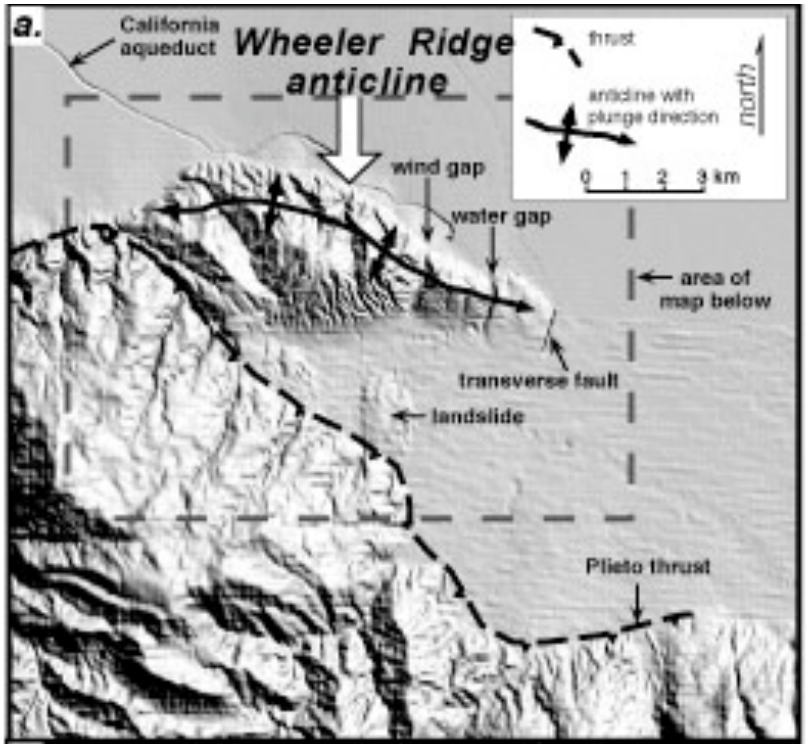

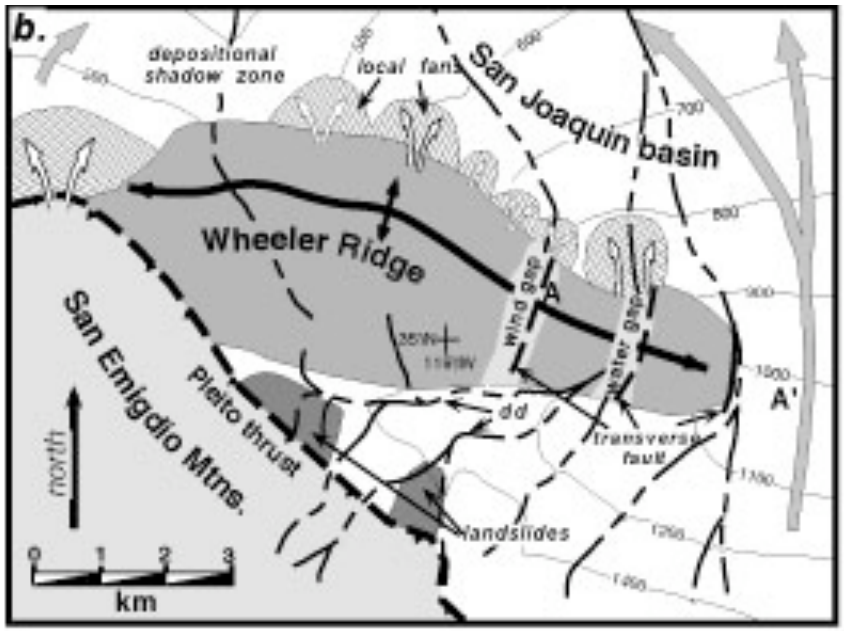

Figure 4.35: Wheeler Ridge, a plunging fold in California.

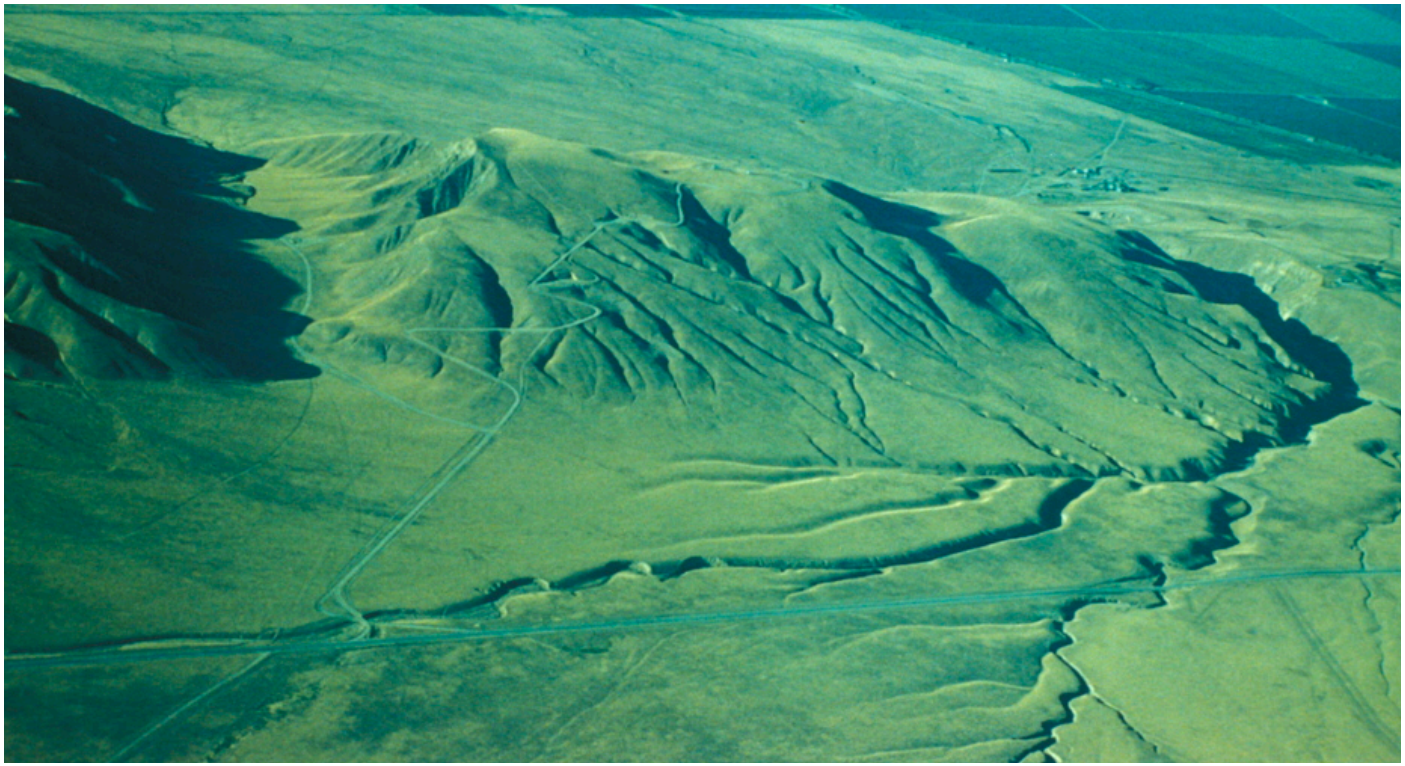

Lateral fold growth above a blind thrust Wheeler Ridge in California

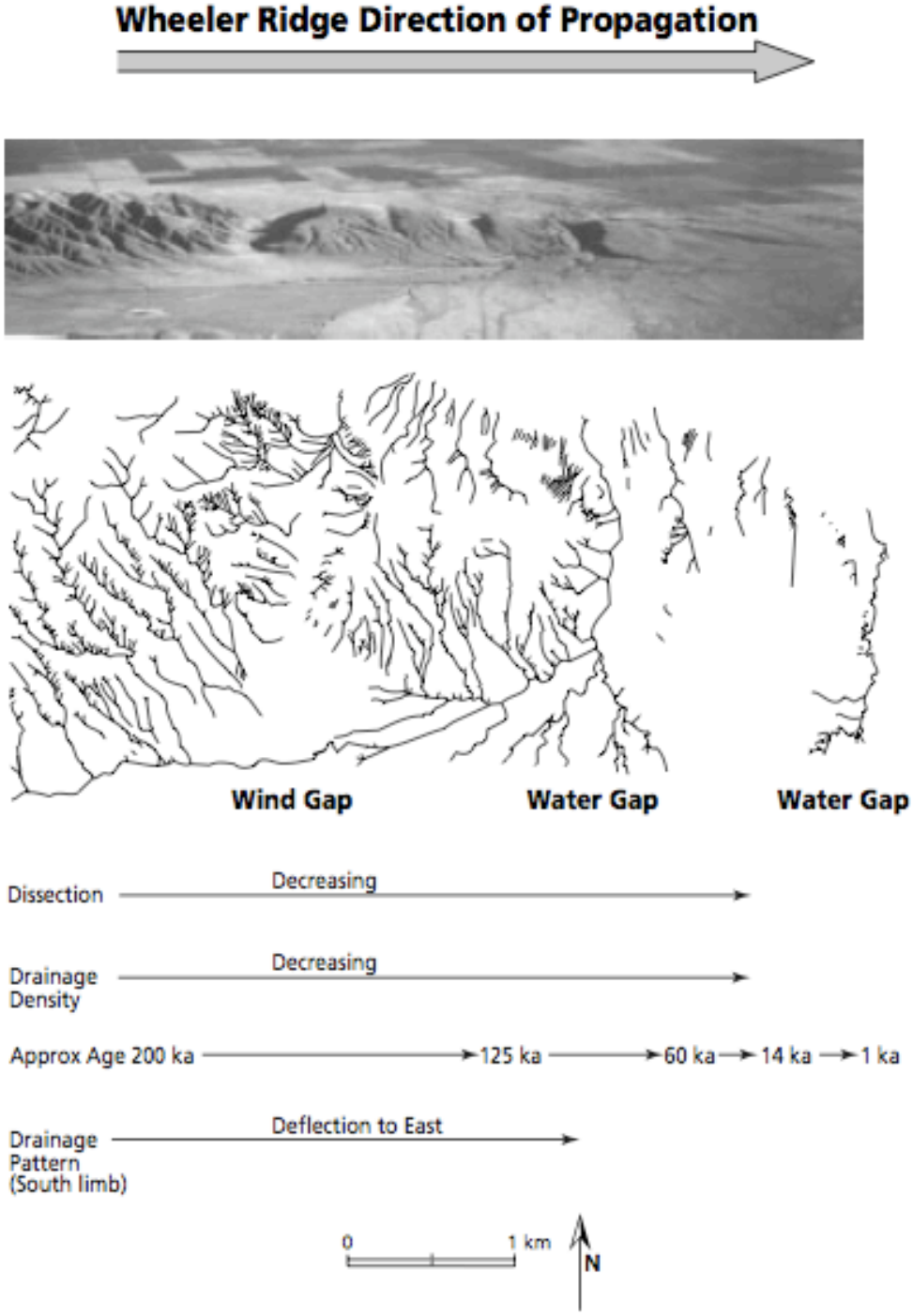

Figure 1. Aerial photograph (courtesy of John S. Shelton), and drainage map of Wheeler Ridge, southern San Joaquin Valley, California (after Keller et al., 1998), illustrating several geomorphic indicators of lateral propagation present at ridge.

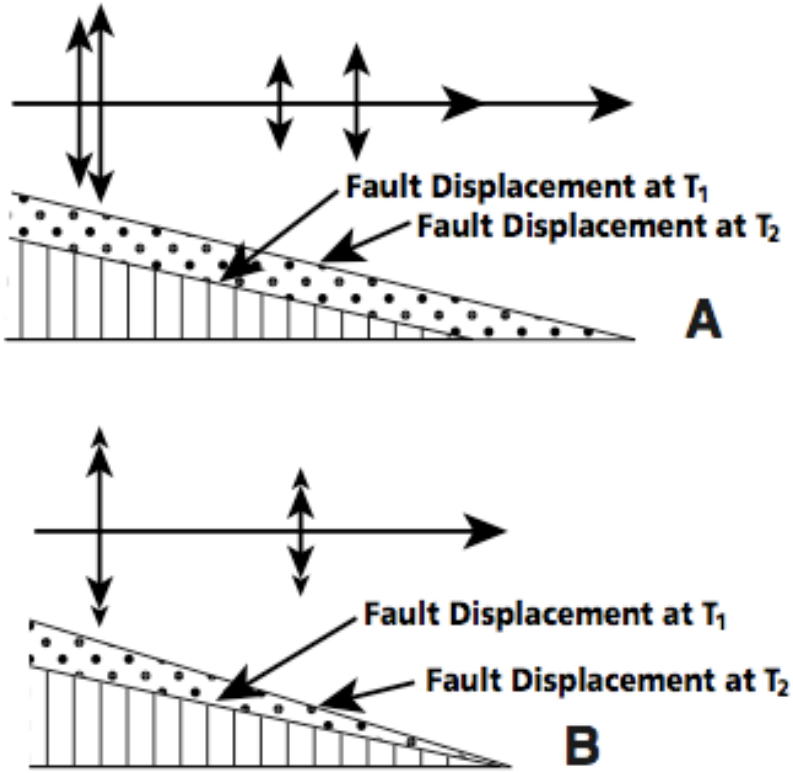

Figure 2. Two models of fold growth. A: Lateral propagation where fault length grows. B: Rotation, where end points of buried fault are fixed. Drawing courtesy of D. Medwedeff.

How can you distinguish between these two scenarios?

Example of fold / fault growth from the Zagros mountains of Iran

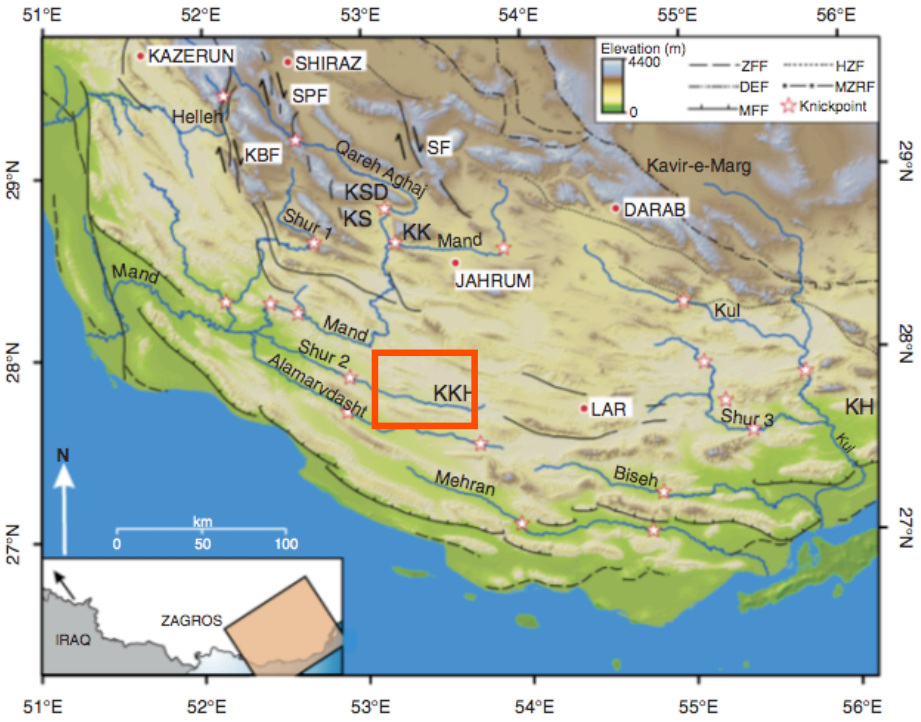

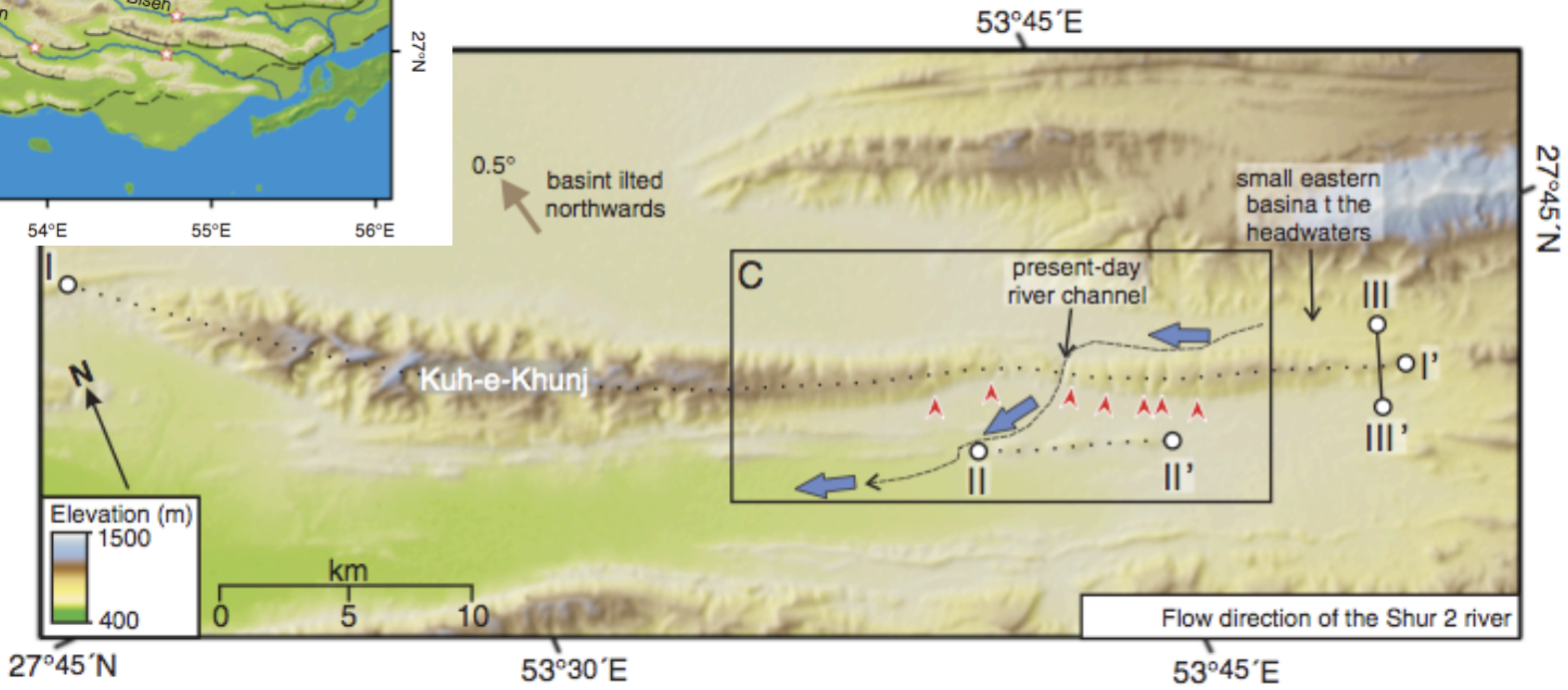

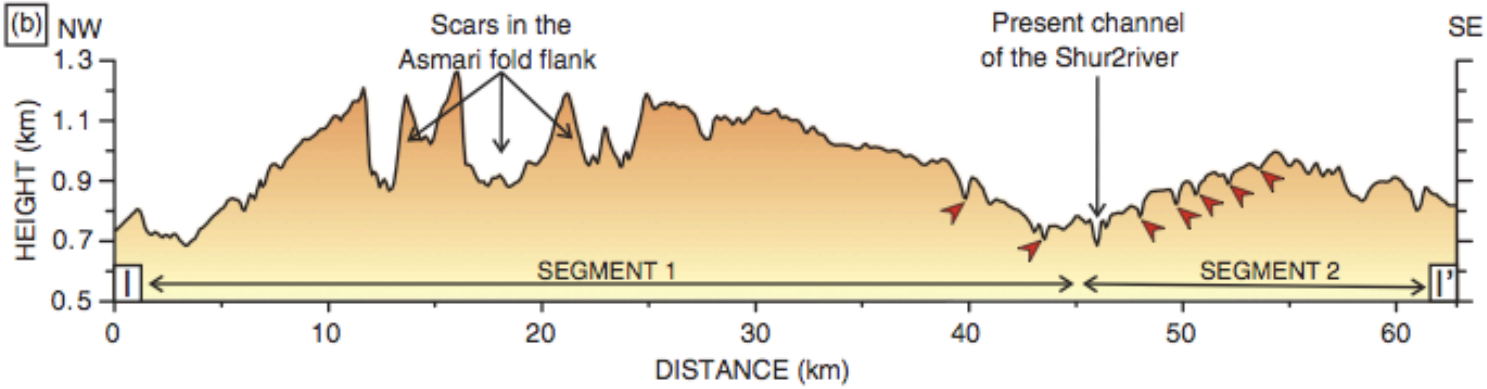

Segment linkage

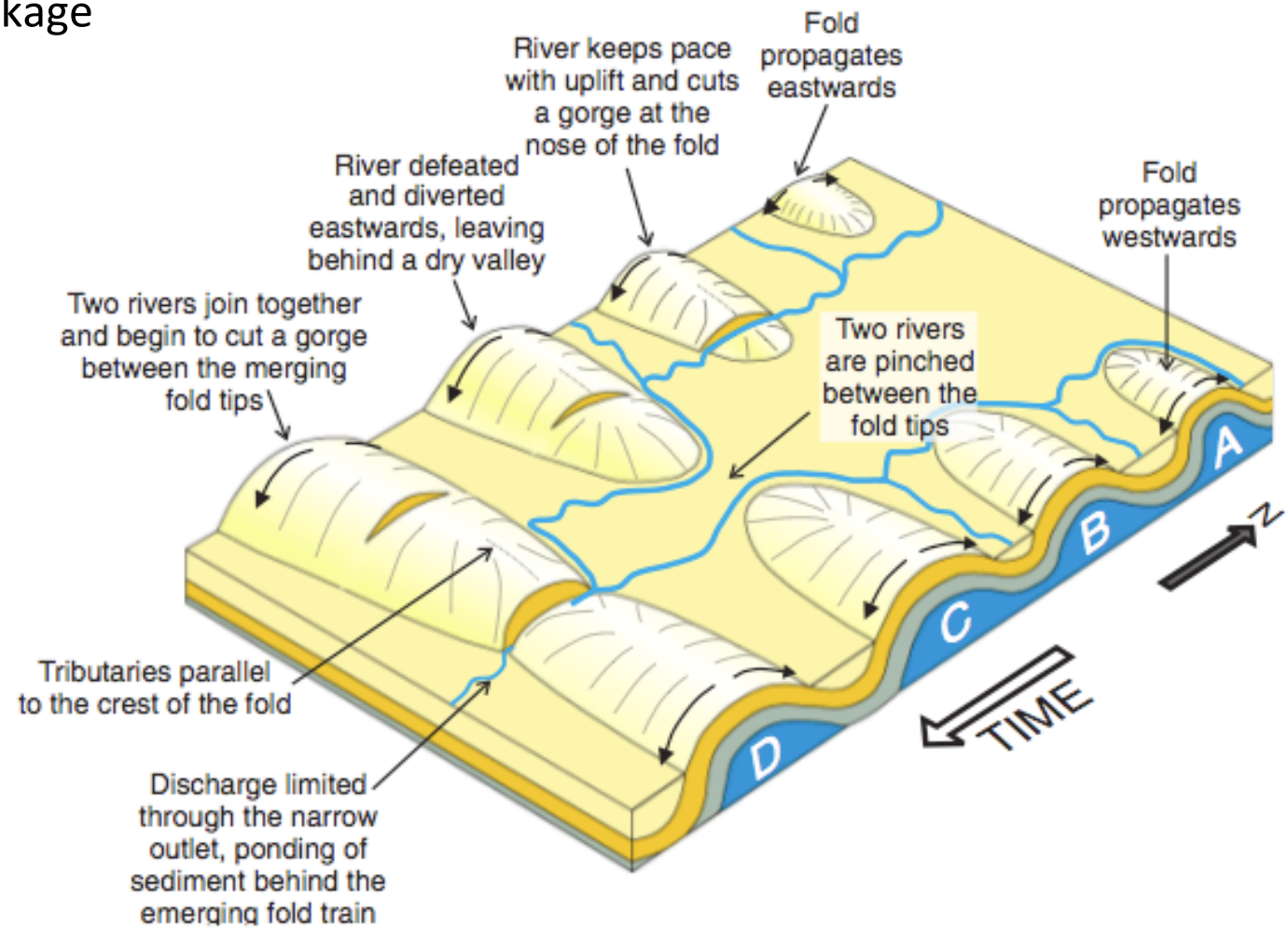

Fig. 11. A cartoon showing the formation of a gorge between two propagating anticlines through time. (a) Two small folds form in the east and west of the landscape. (b) The folds propagate towards one another. Growth on aligned fold segments is enhanced by positive feedback in the stress changes around each growing fold (Cowie, 1998). The incision rate of the western river keeps pace with uplift and the river incises a gorge through the nose of the fold. (c) The western river is unable to keep pace with uplift and the gorge is abandoned and left as a dry valley. The river is diverted to the east and pinched between the tips of the two folds. (d) The folds continue to propagate towards one another and the tips of the folds begin to form a continuous structure. The rivers have increased their stream power by joining together and incise a gorge through the almost continuous anticline. The narrowed outlet prevents the efficient removal of sediment from the basin. A tributary pattern parallel to the crest of the fold is inherited from an earlier stage of growth.

Segment linkage

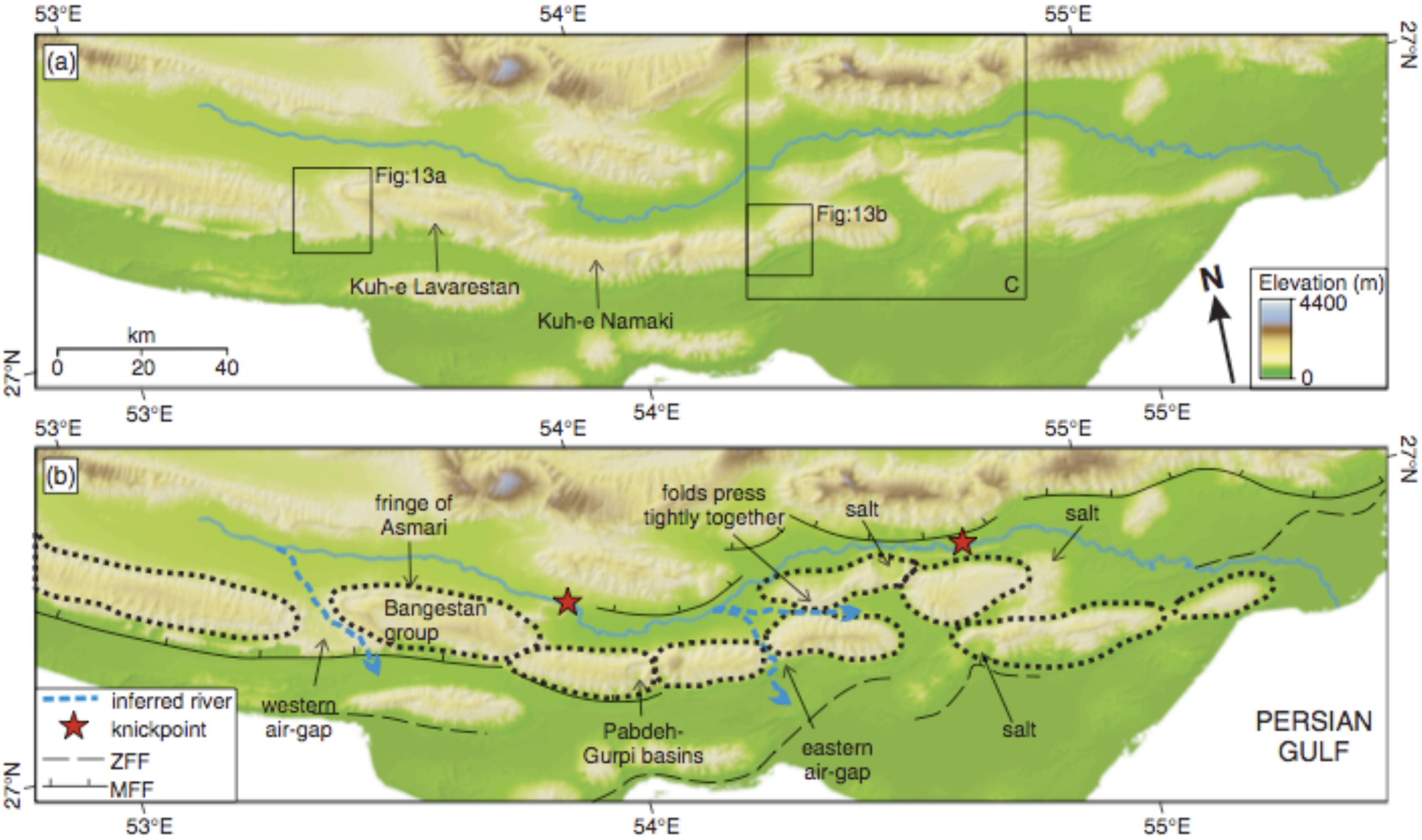

Ground rupture in a reverse faulting earthquake

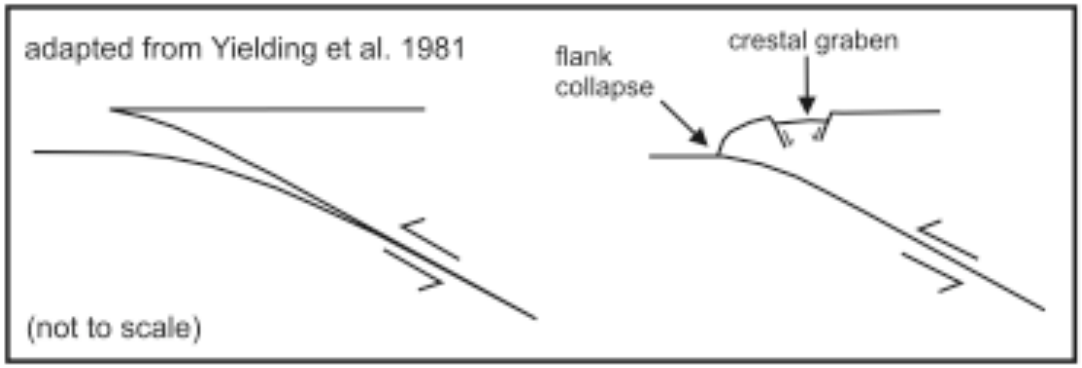

Fig. 50. (a) Part of the reverse fault coseismic ruptures from the M_s 7.3 El Asnam earthquake in Algeria, looking towards the uplifted hanging wall. On the right is a very rare example of an exposed striated shear surface. Much more common is for the overhanging block to collapse, as on the left [see Fig. 26(b)]. (b) Part of the coseismic thrust fault ruptures on Tüleet Uul, following the 1967 Mogod (M_w 7.1) earthquake in Mongolia [Baljinnyam *et al.*, 1993; Bayasgalan and Jackson, 1999]. The fault dips to the left at ~30°, but at the surface produced a collapsed free face 2–3 m high [Fig. 26(b)].

Sabzevar

Fattahi et.al. 2006

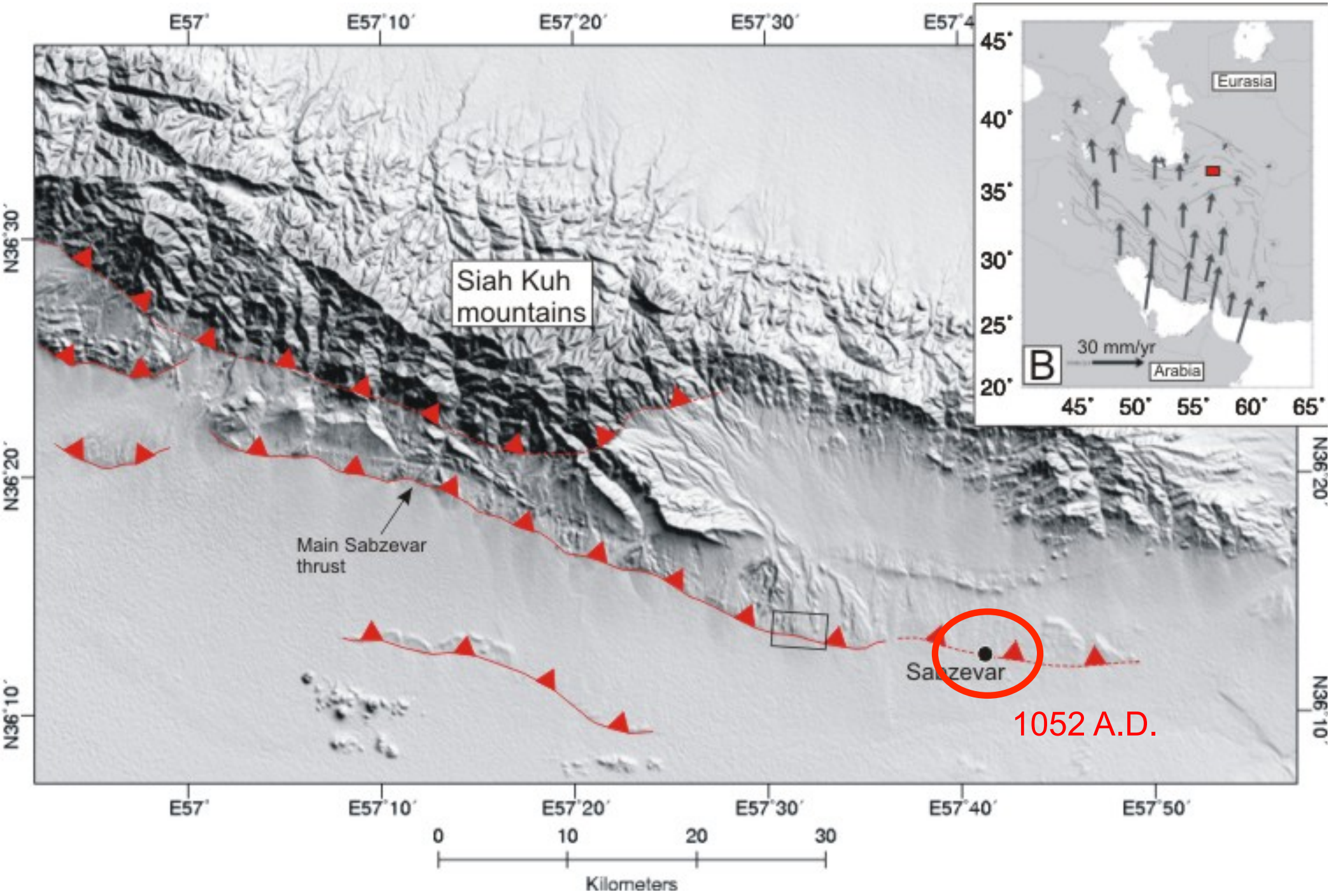

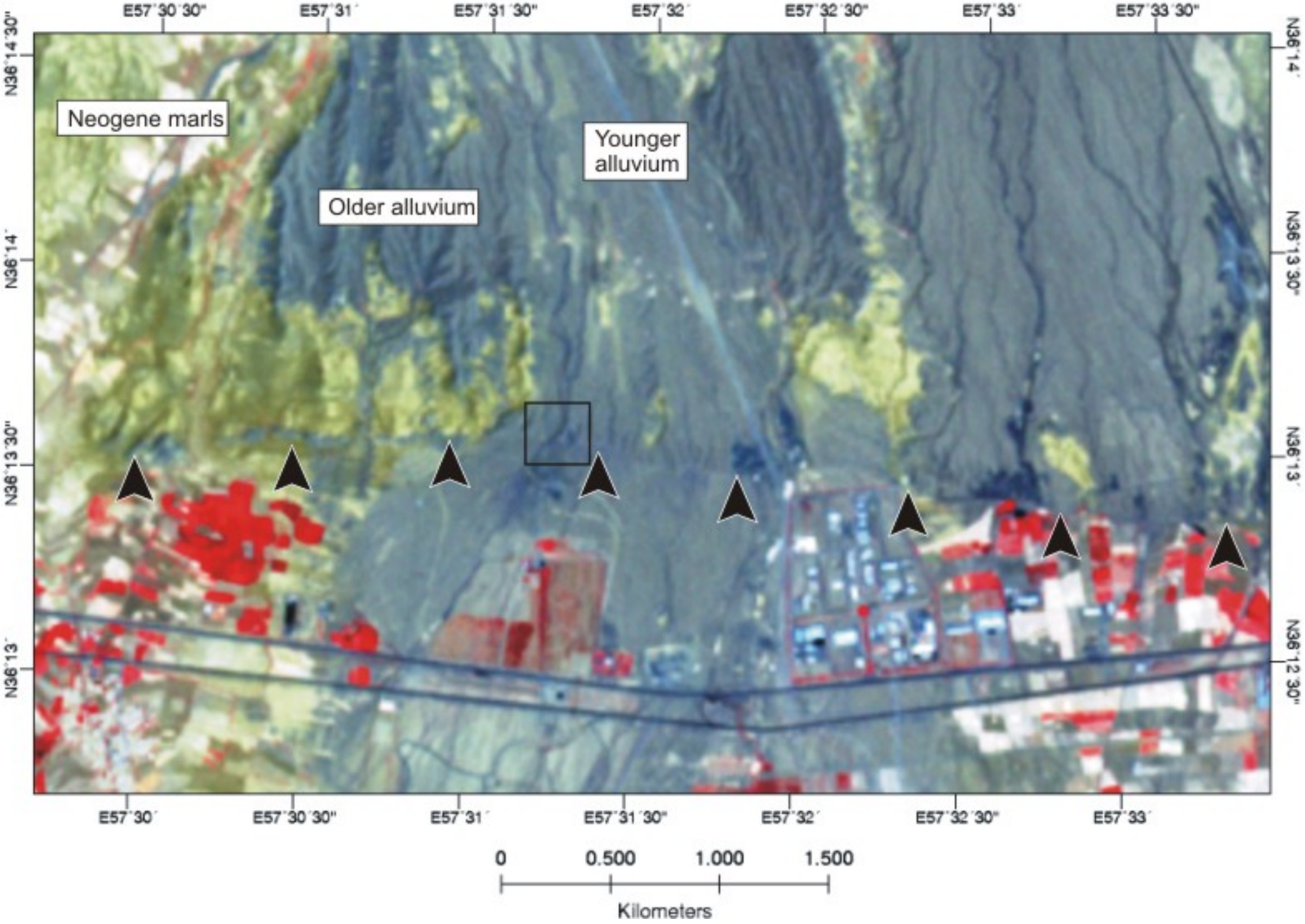
E57°30'30"
E57°31'
E57°31'30"
E57°32'
E57°32'30"
E57°33'
E57°33'30"
N36°14'30"
N36°14'
N36°13'30"
N36°13'
N36°12'30"
Neogene marls
Younger alluvium
Older alluvium
E57°30'
E57°30'30"
E57°31'
E57°31'30"
E57°32'
E57°32'30"
E57°33'
0
0.500
1.000
1.500
Kilometers

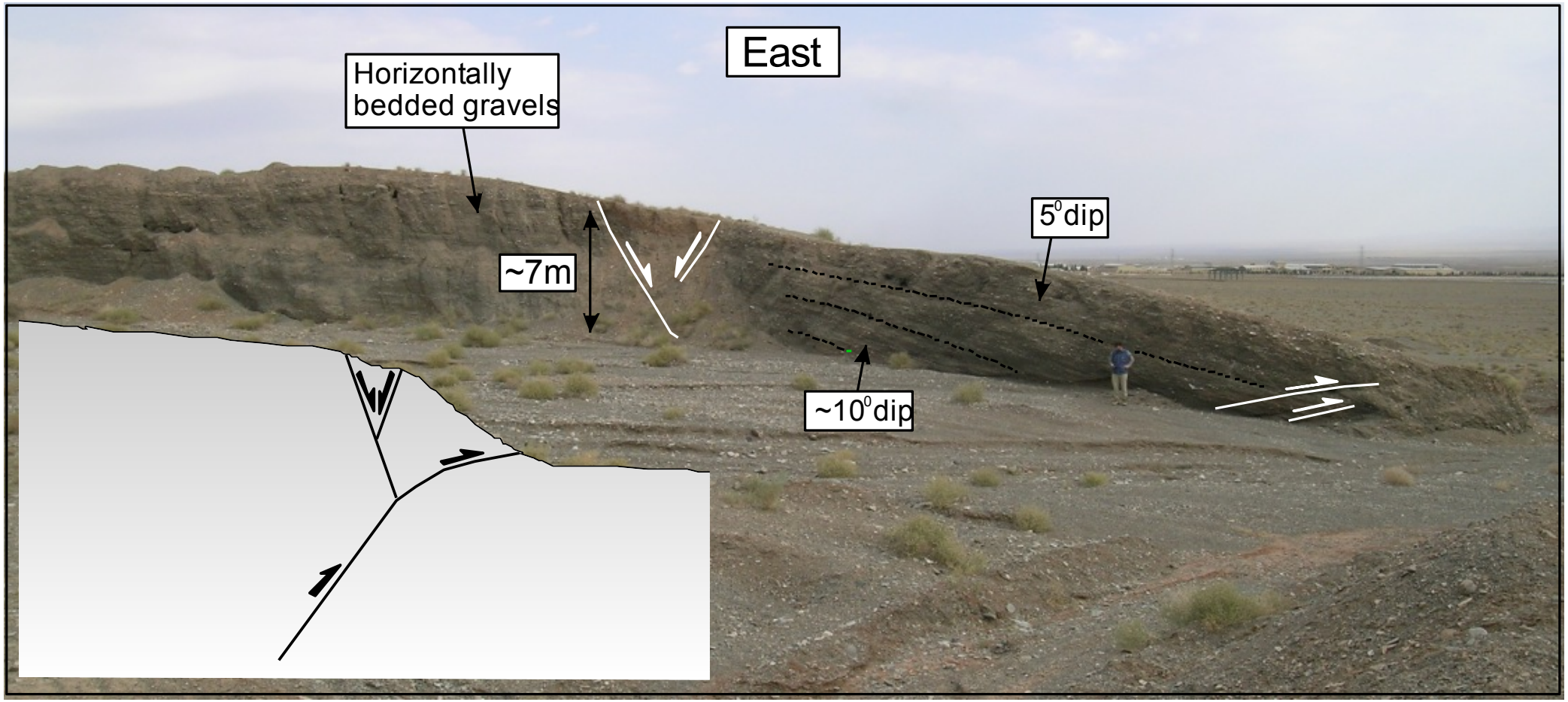
East
Horizontally bedded gravels
~7m
5⁰dip
~10⁰dip

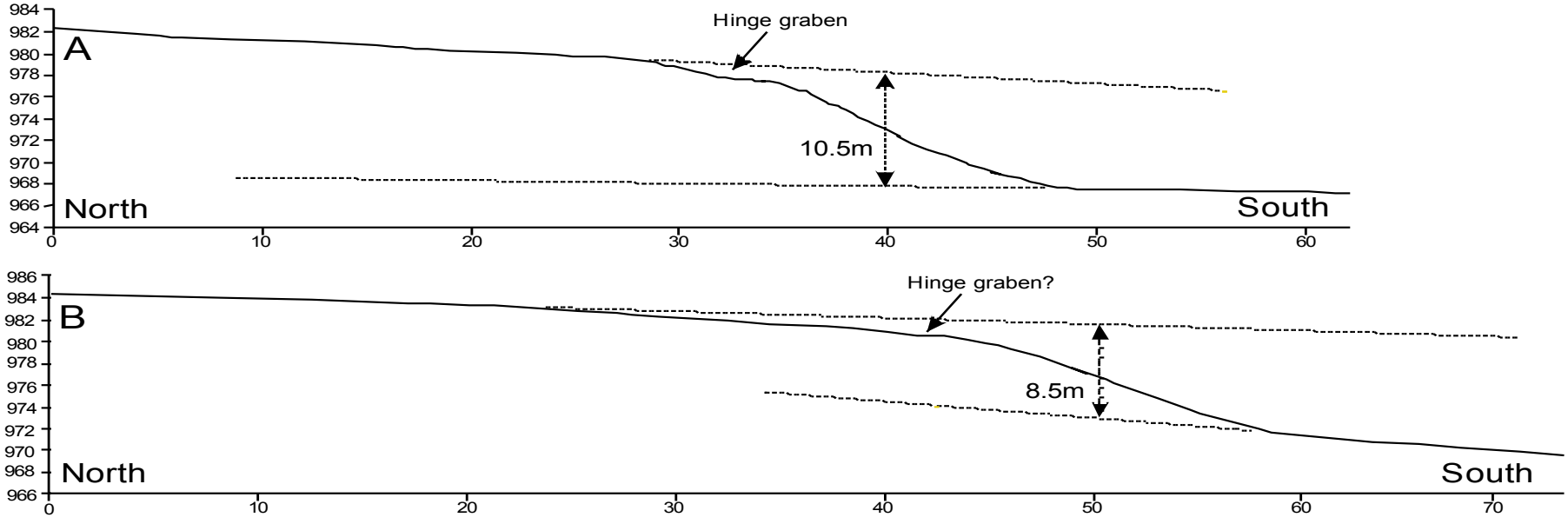
A
Hinge graben
10.5m
North
South
984
982
980
978
976
974
972
970
968
966
964
0
10
20
30
40
50
60
B
Hinge graben?
8.5m
North
South
986
984
982
980
978
976
974
972
970
968
966
0
10
20
30
40
50
60
70

Optically-Stimulated Luminescence dating

- Sample in the dark
- Measure the ‘dose’
- Are the samples ‘re-set’

Photos by J. Hollingsworth

Sabzevar reverse fault

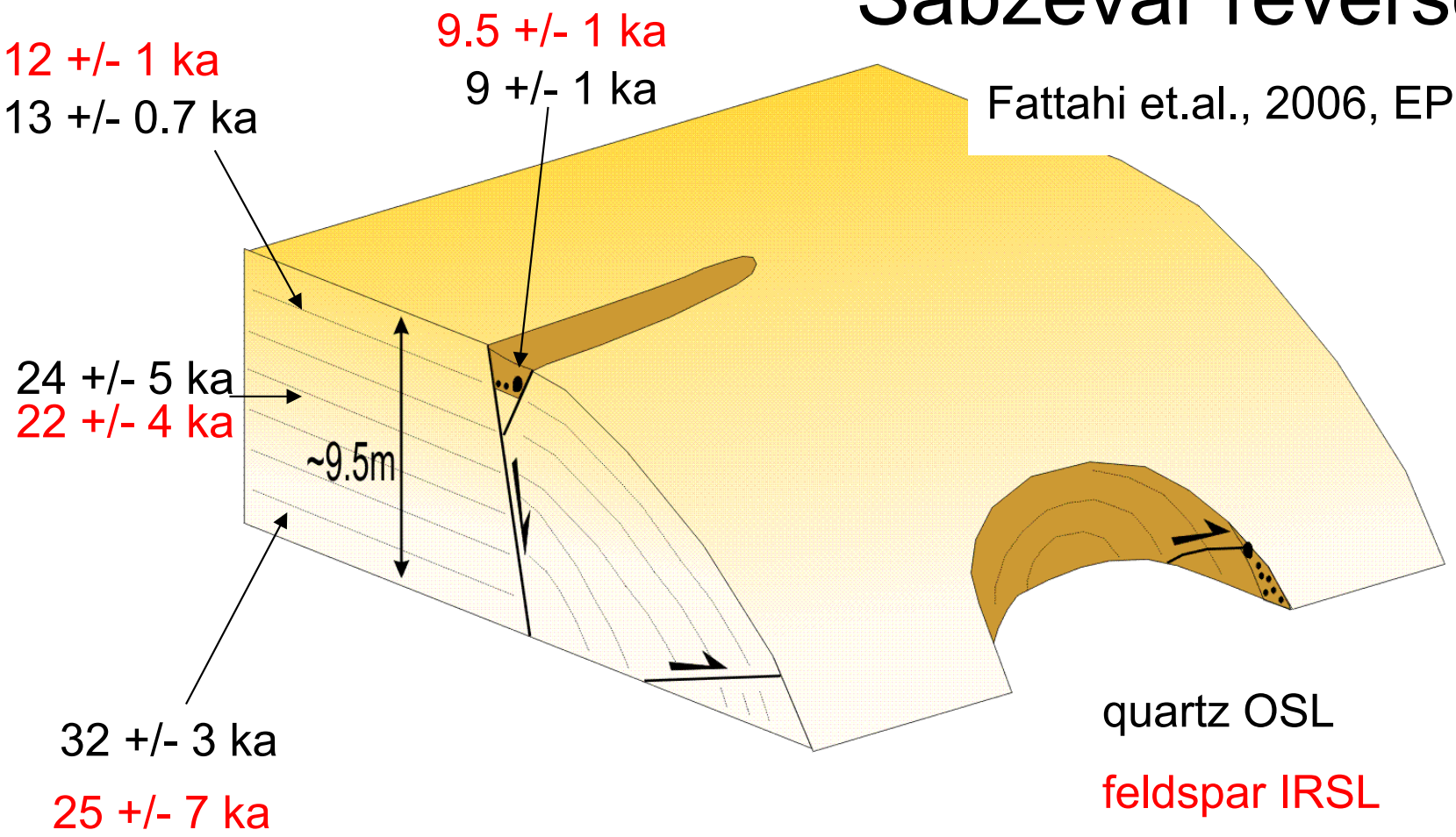

Fattahi et.al., 2006, EPSL

quartz OSL

feldspar IRSL

Alluvial deposition from ~30 to 10 ka

– followed by river incision

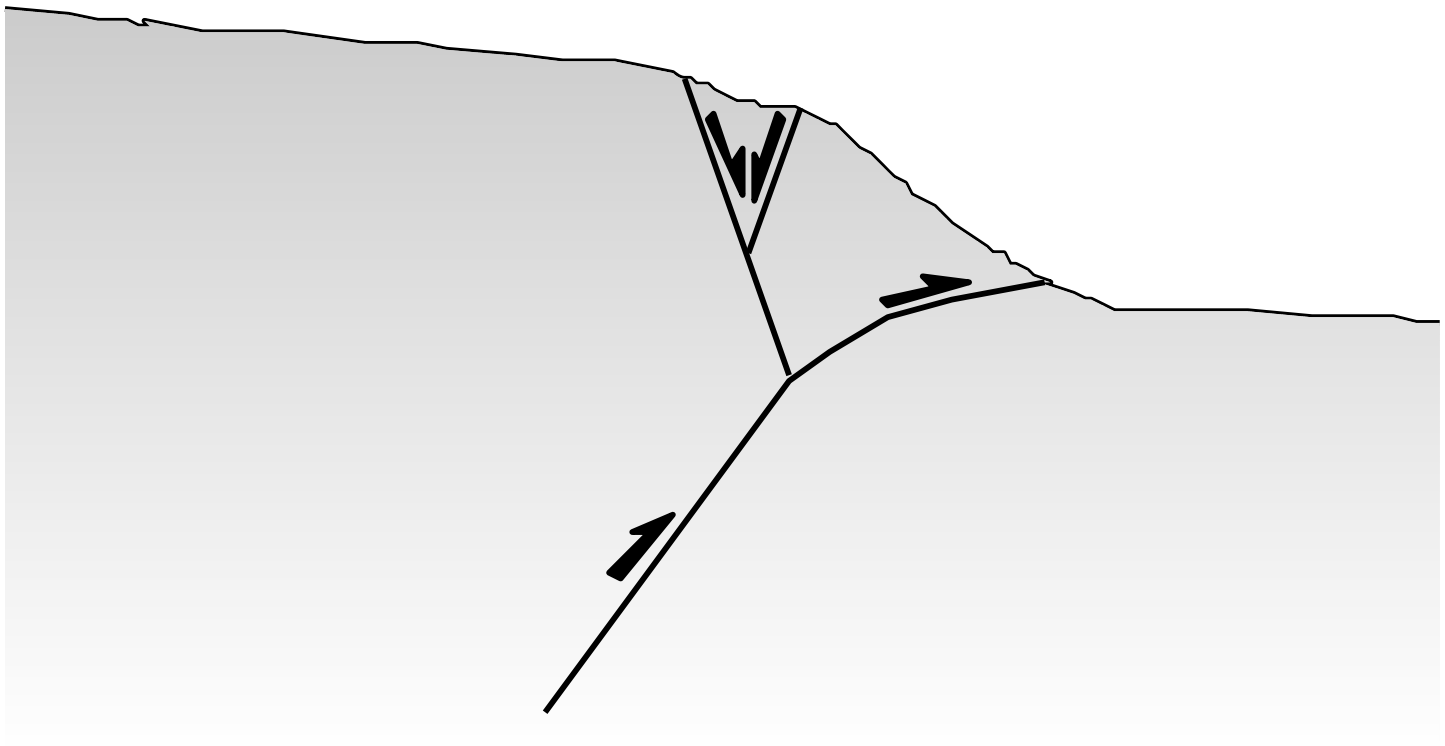

~ 9.5m Uplift in ~10-12 ka

Shortening ~0.4-0.6 mm/yr

Slip-rate ~1 mm/yr

M7 earthquake repeat time ~3000 years

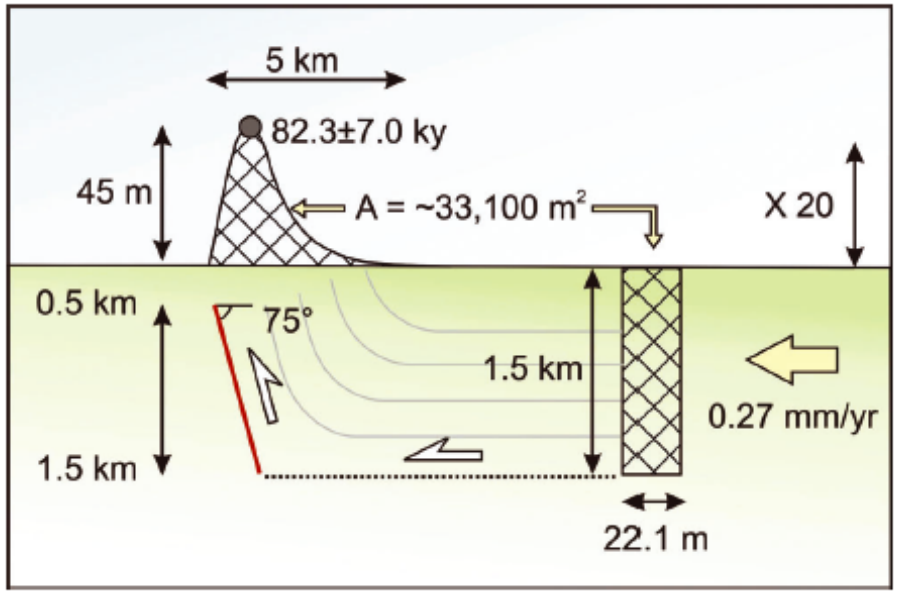

Palaeoseismology of ground-rupturing thrust earthquakes

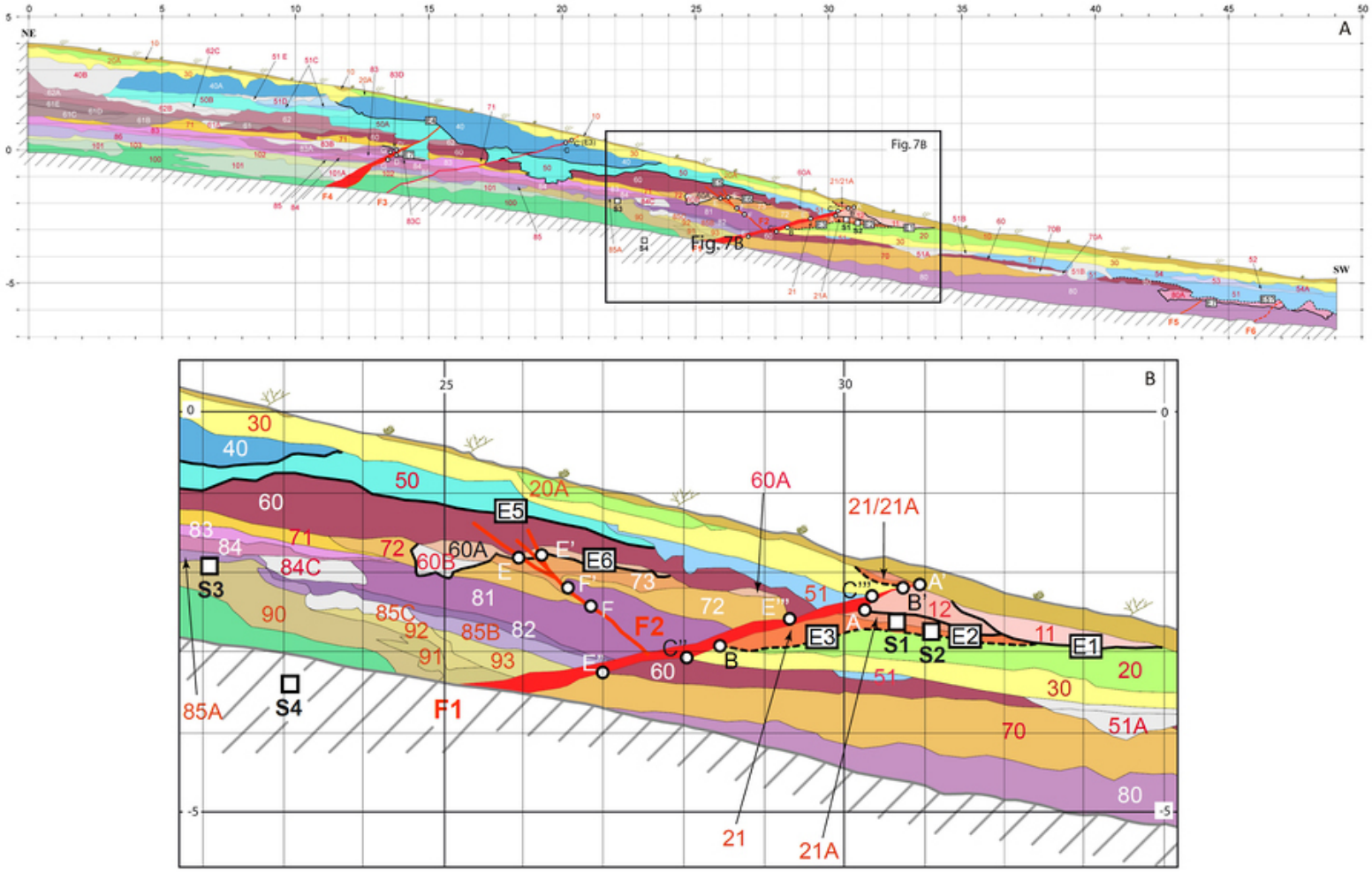

Journal of Geophysical Research: Solid Earth
Volume 117, Issue B6, B06305, 7 JUN 2012 DOI: 10.1029/2012JB009147
http://onlinelibrary.wiley.com/doi/10.1029/2012JB009147/full#jgrb17217-fig-0007

(a)

Fig. 27. (a) A normal fault on the crest of the hanging wall anticline ridge (Sera el Maarouf) above the reverse fault that moved in the 1980 El Asnam earthquake (M_s 7.3) in Algeria [see Fig. 26(c)]. Note how the top 50 cm has failed in tension, while the lower part has failed in shear on a striated surface (see Fig. 37). Photo courtesy G. Yielding. (b) A minor normal fault in the relay or step position between two large faults segments [see Fig. 26(a)]. This N–S fracture was formed between the E–W segments 5 and 6 of the Platea-Kaparelli fault system (Fig. 28) that moved in the 4 March 1981 earthquake in the eastern Gulf of Corinth, Greece. (c) Aerial view looking north across the Perakora peninsula in the eastern Gulf of Corinth (Fig. 28). The numerous ridges on the peninsula, including the one bounding the lagoon, which is about 200 m high and 2 km long, are all small normal faults between the large fault segments bounding Mt. Gerania and the deep basin offshore from Kiato. Some of them moved in the 1981 earthquake sequence [Fig. 27(d)]. (d) A small fault at Milokopi (segment 4 in Fig 28) on the Perakora peninsula, which moved about 10 cm over a length of ~1 km in the 1981 earthquakes. The 1981 rupture consisted of a small tensional fracture in the grass-covered alluvium and scree about 1 m in front of the standing figure and about 10 m in front of the shear surface on the fault itself, which makes the reflective plane in the background. (c.f. Fig. 37).

If the fault is 'blind', crestal normal faults and fissures might be all you see …

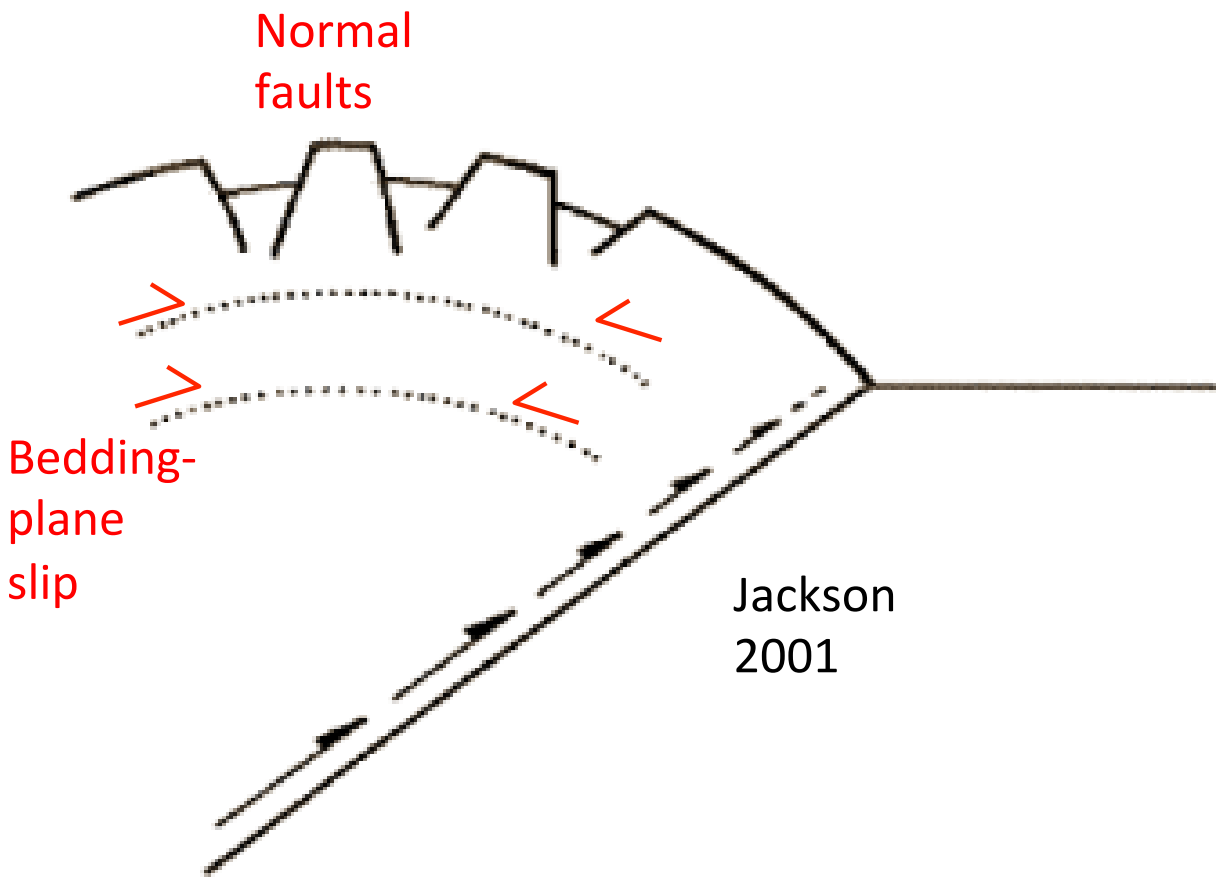

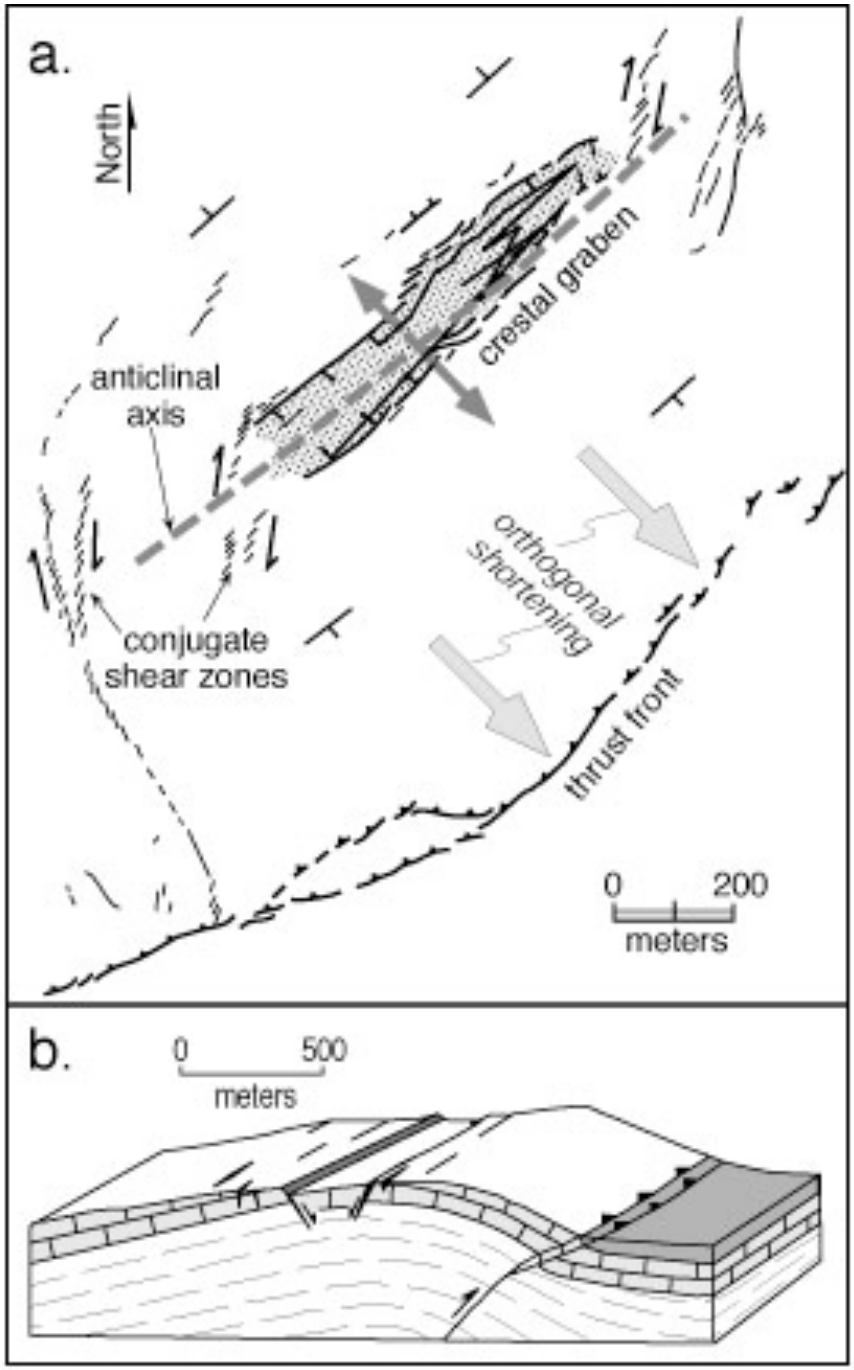

Figure 4.28: El Asnam thrust front and crestal graben

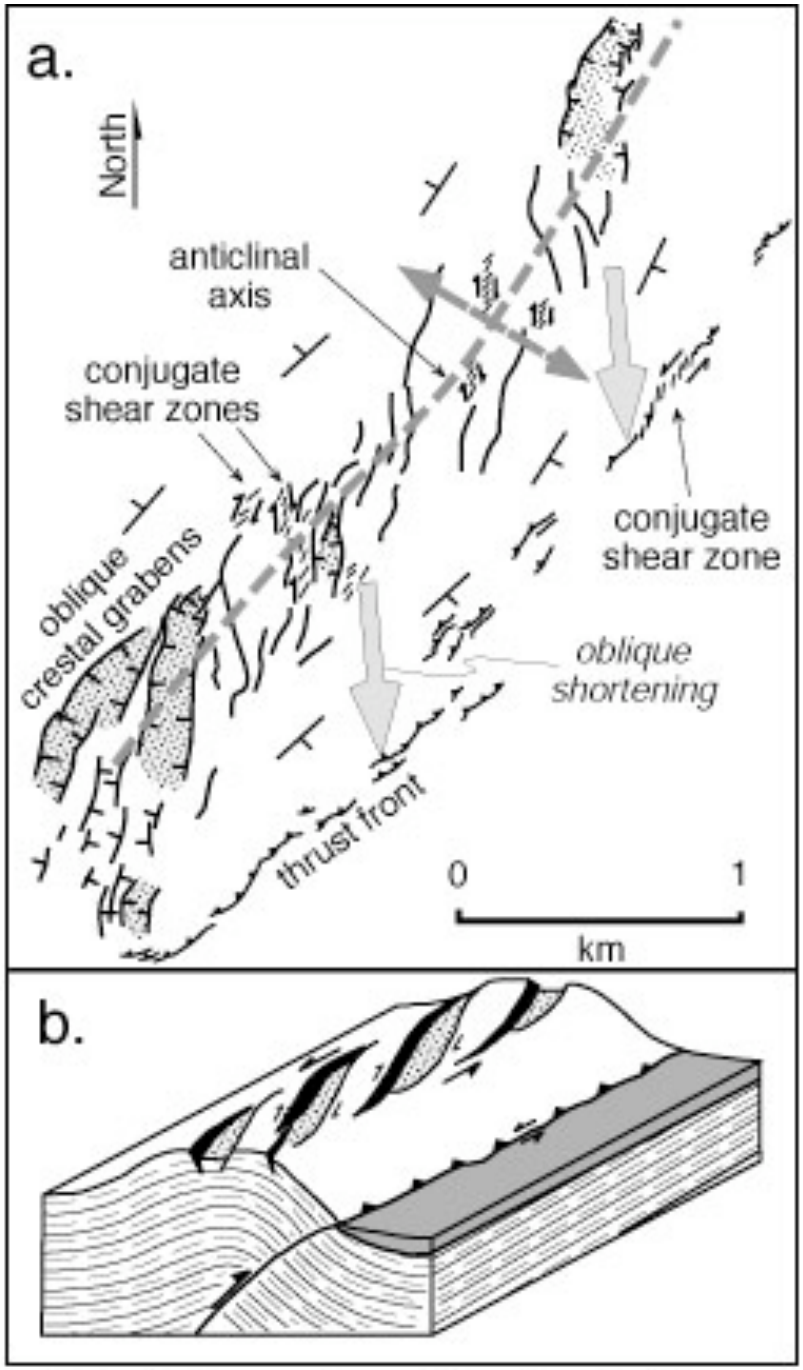

Figure 4.29: El Asnam thrust front and oblique grabens.

- measuring slip-rate of reverse faults

- to work out the shortening, need to know how dip varies with depth

- If fault is blind, makes it even more challenging (note that could be some folding even if ruptures surface).

Tabas

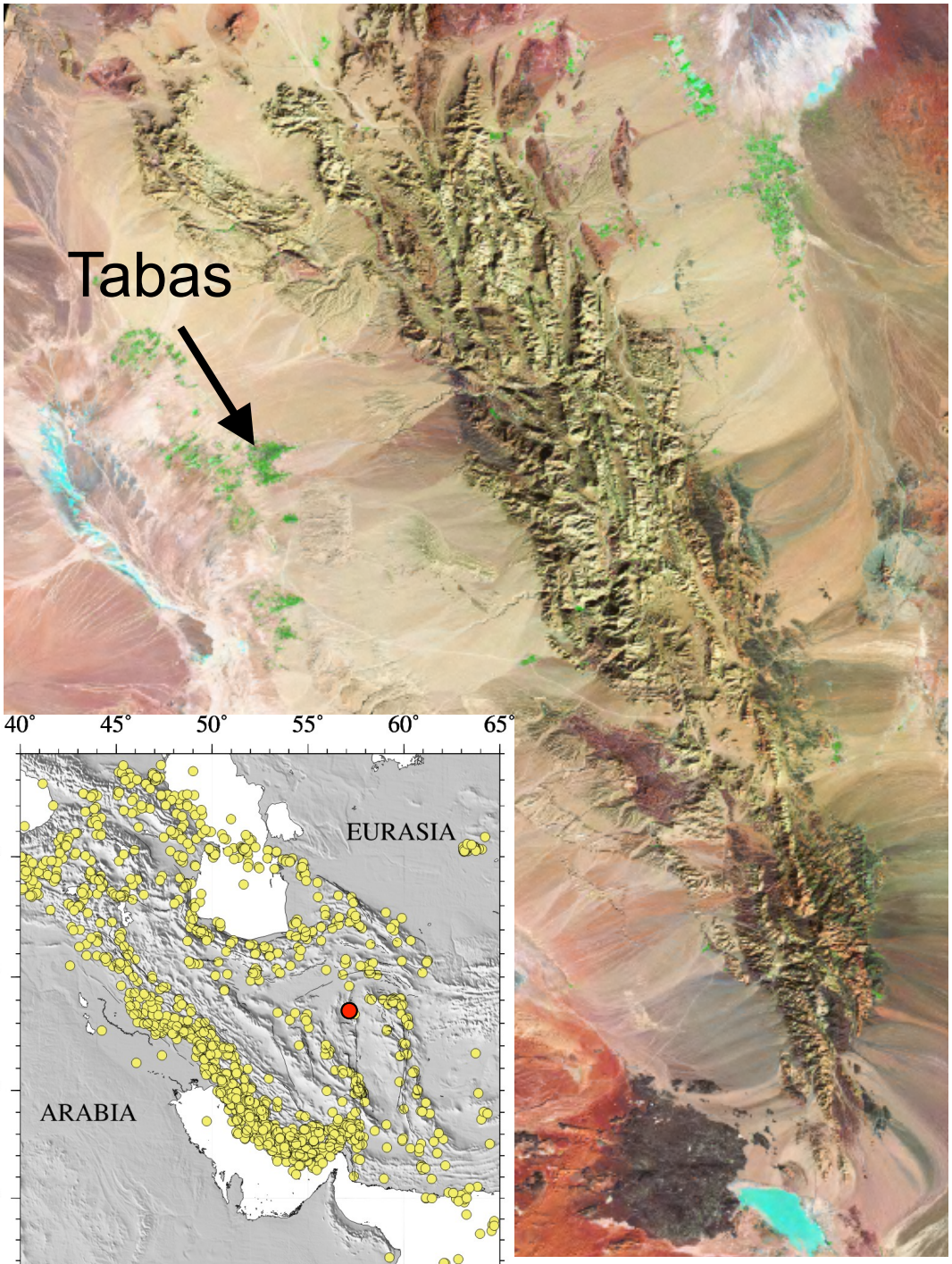


13,000 population;
11,000 killed (85%)
Tabas-e-Golshan, 1978 (M_w 7.3)

Tabas

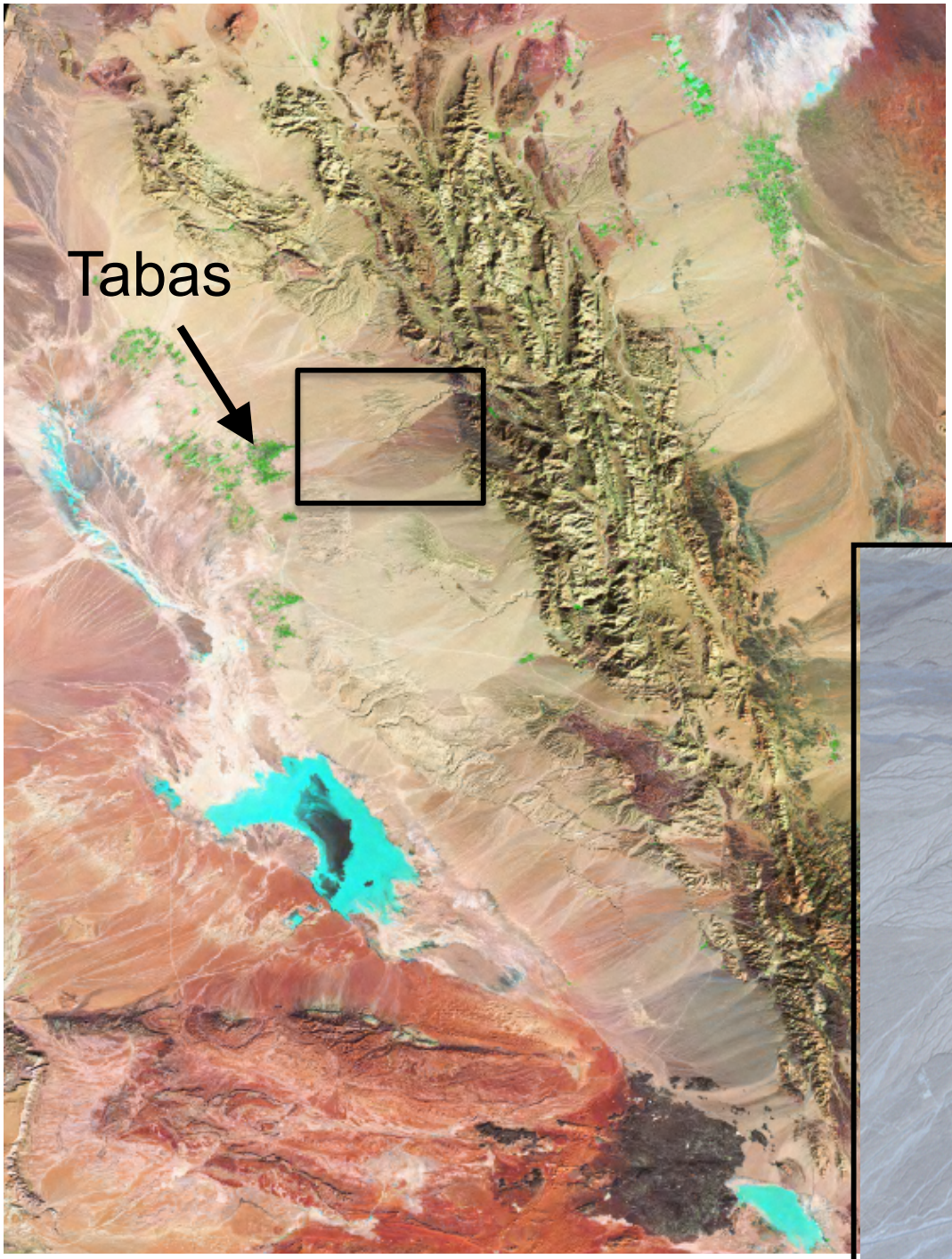

- 16th September 1978
- Magnitude 7.4
- 20,000 deaths (85% of the population!)

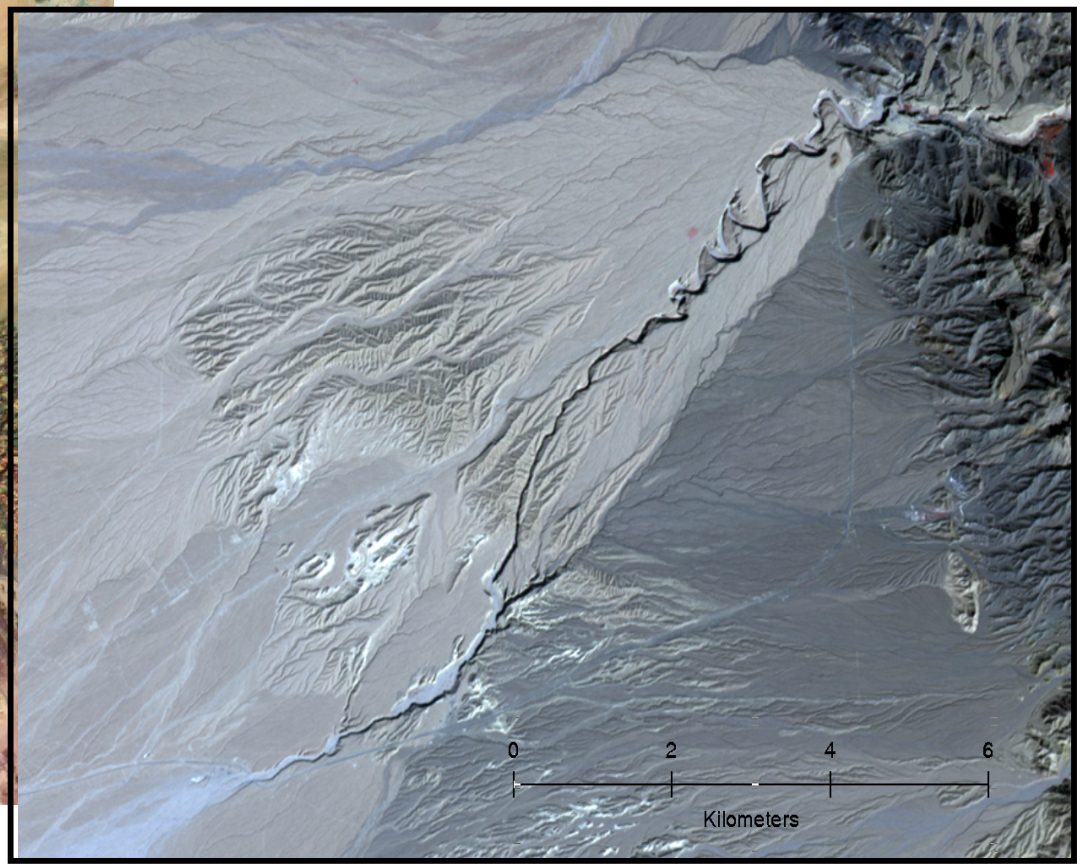

Using GoogleEarth

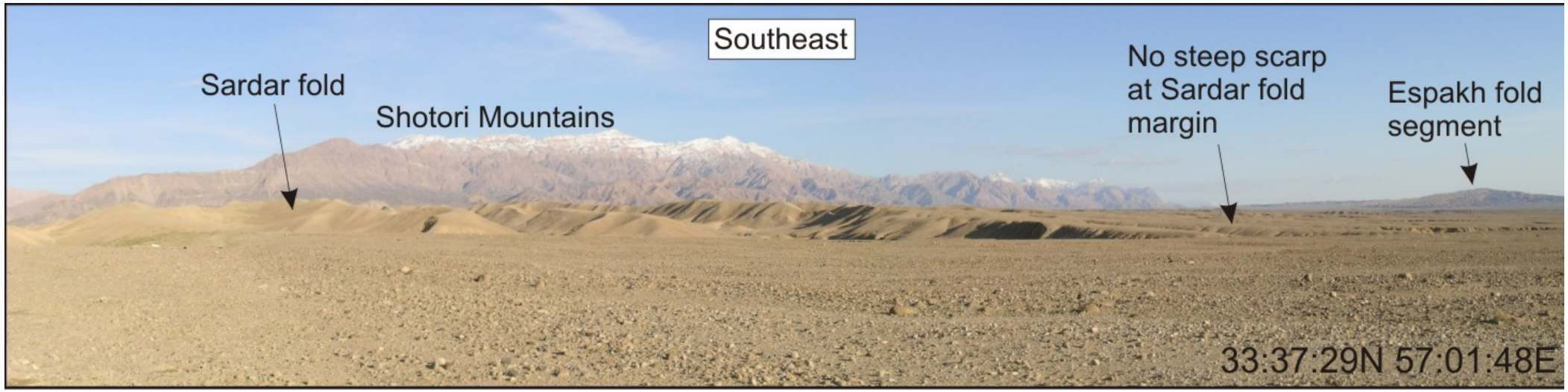
Southeast
Sardar fold
Shotori Mountains
No steep scarp
at Sardar fold
margin
Espakh fold
segment
33:37:29N 57:01:48E

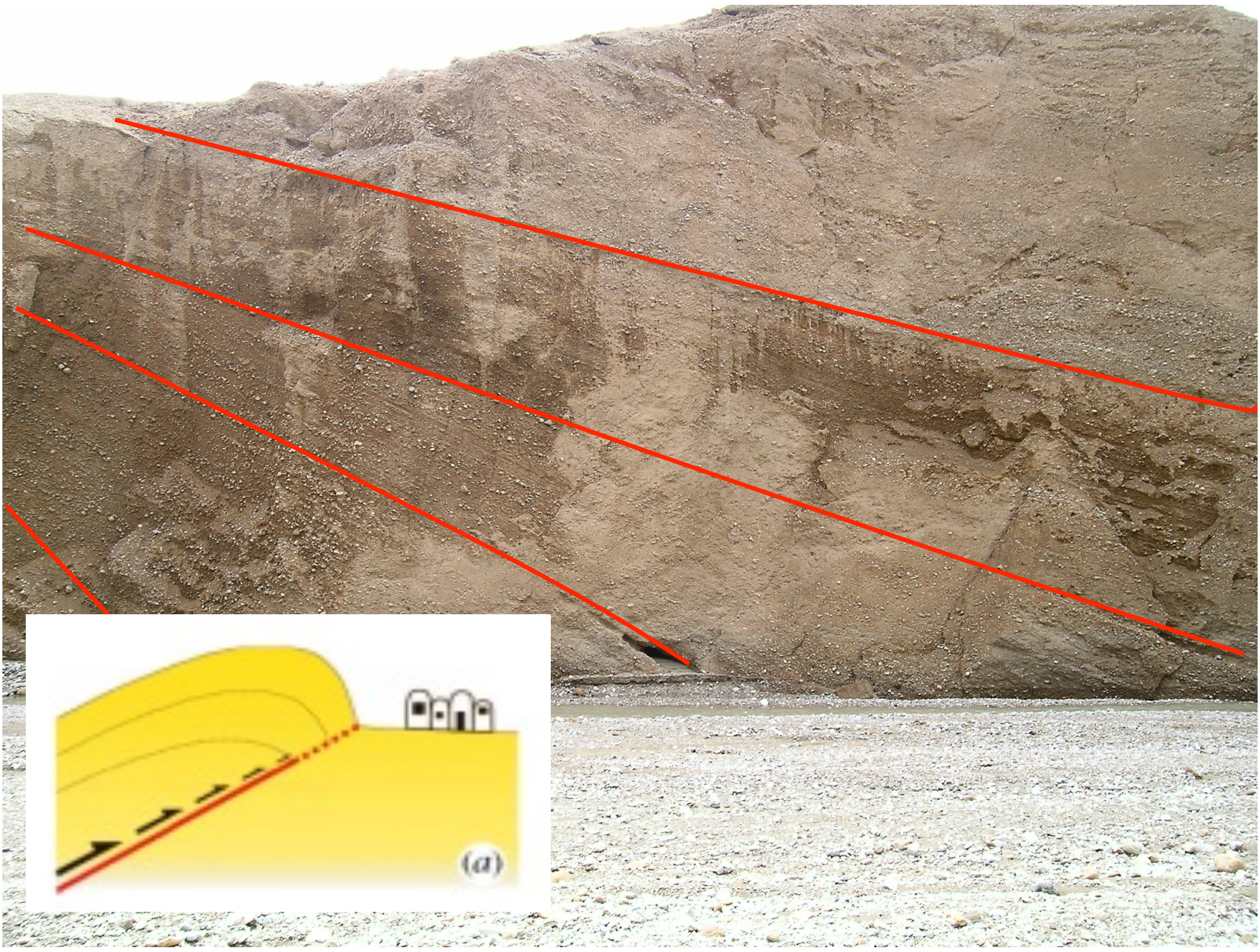
(a)

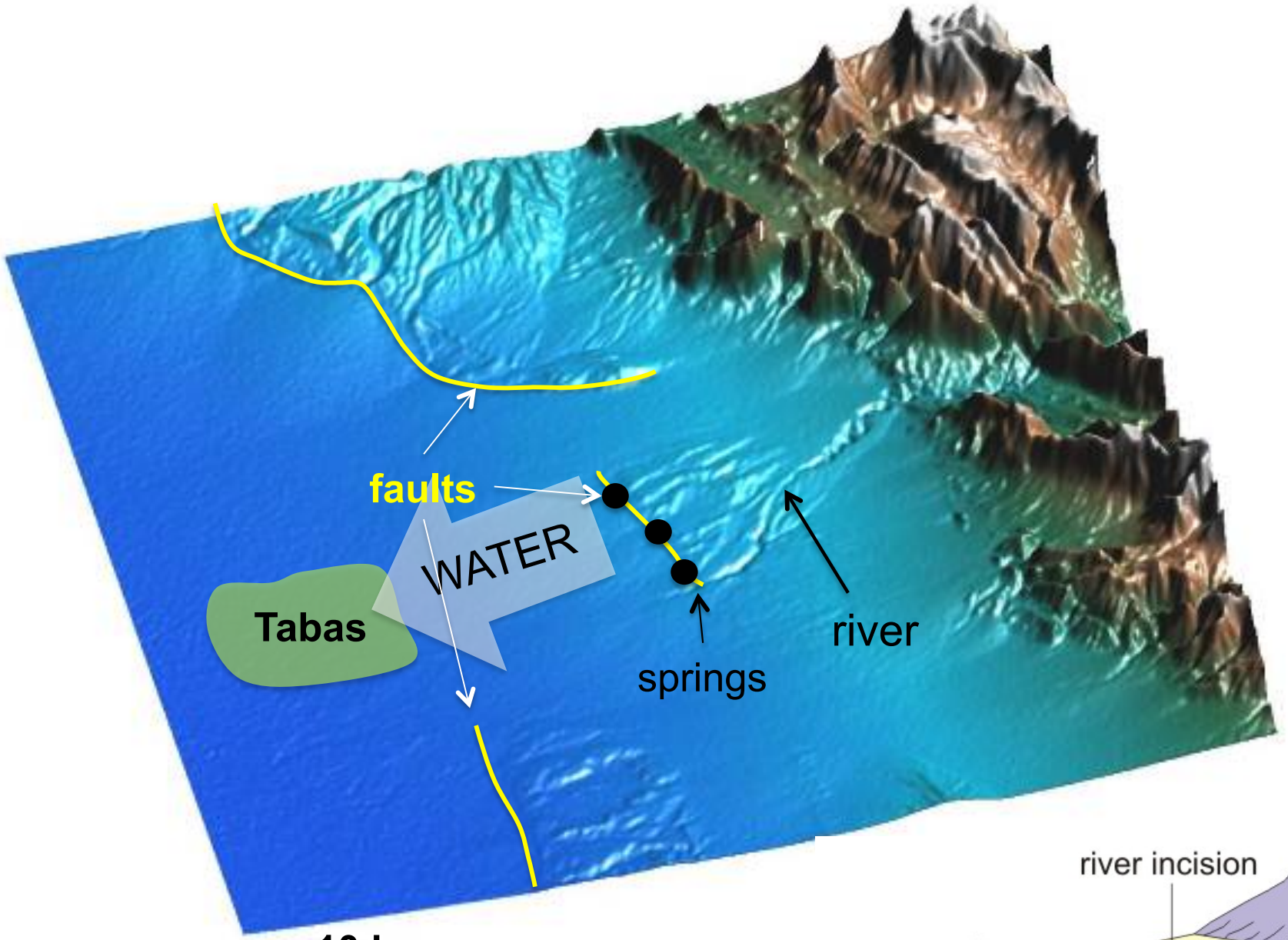

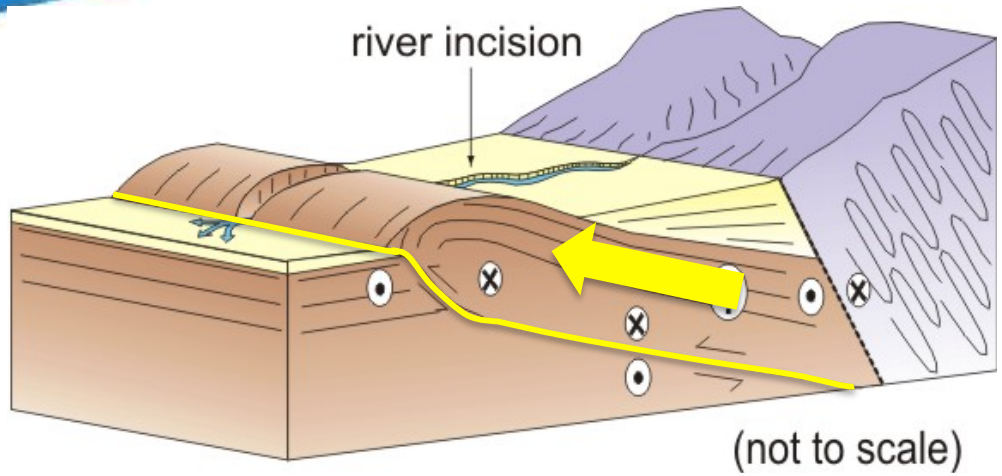

J. Hollingsworth & M.J. Bolourchi

Blind thrust faults
(those that don't reach the Earth's surface)

Manuel Berberian

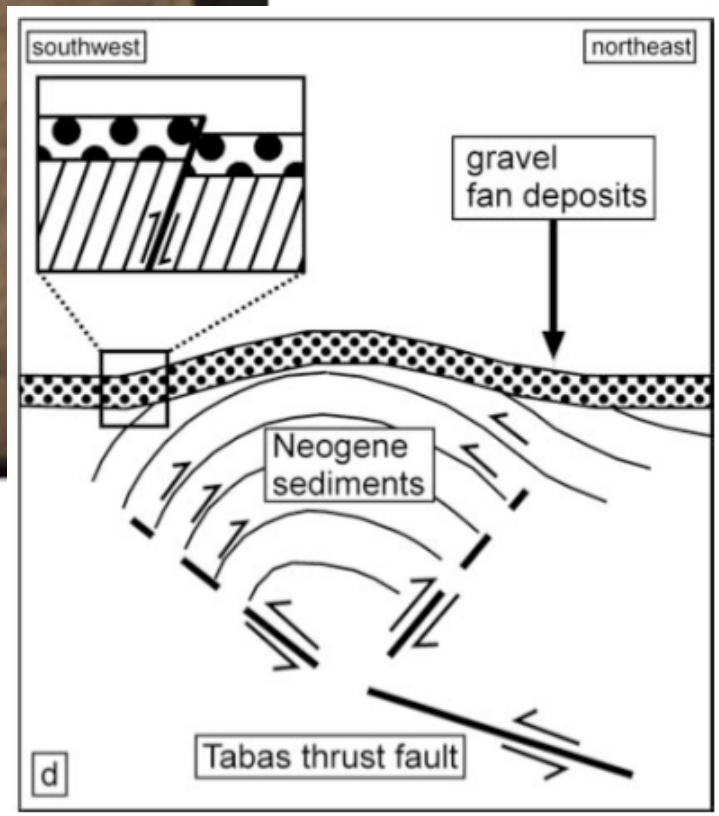

Example: The 1978 Tabas earthquake,
E. Iran (Walker et.al. 2003)

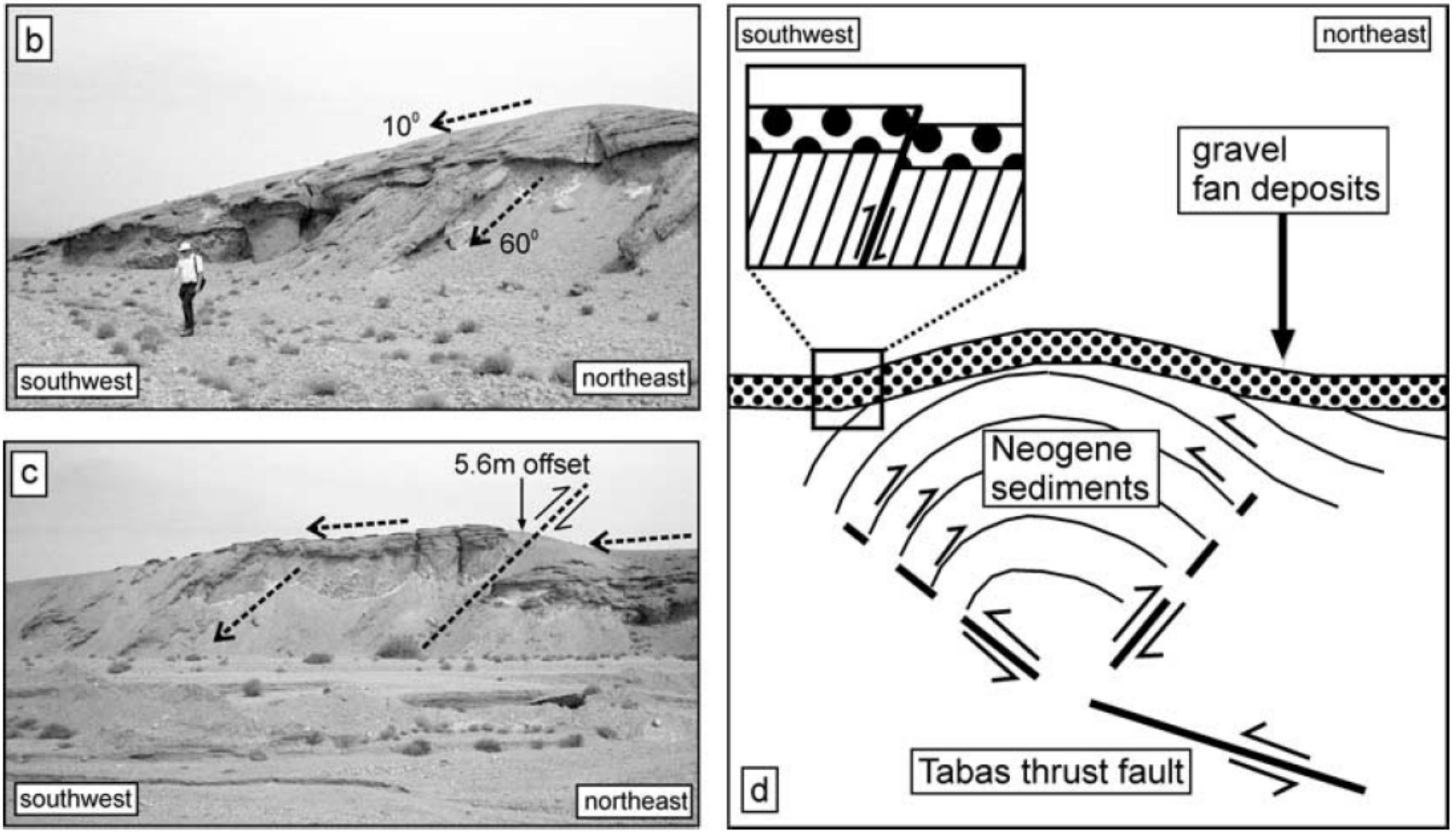
b
10°
60°
southwest
northeast
c
5.6m offset
southwest
northeast
southwest
northeast
gravel
fan deposits
Neogene
sediments
Tabas thrust fault
d

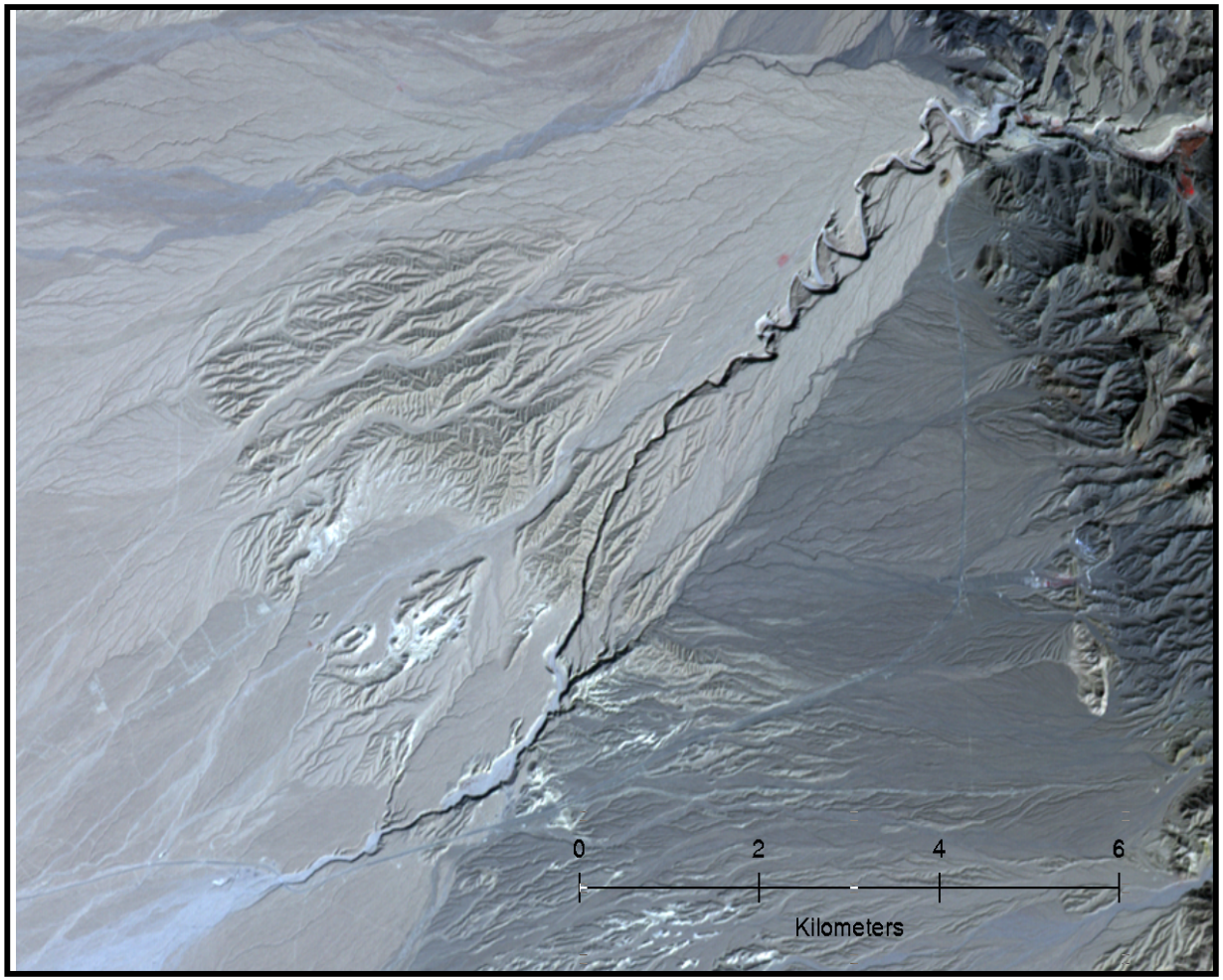
0
2
4
6
Kilometers

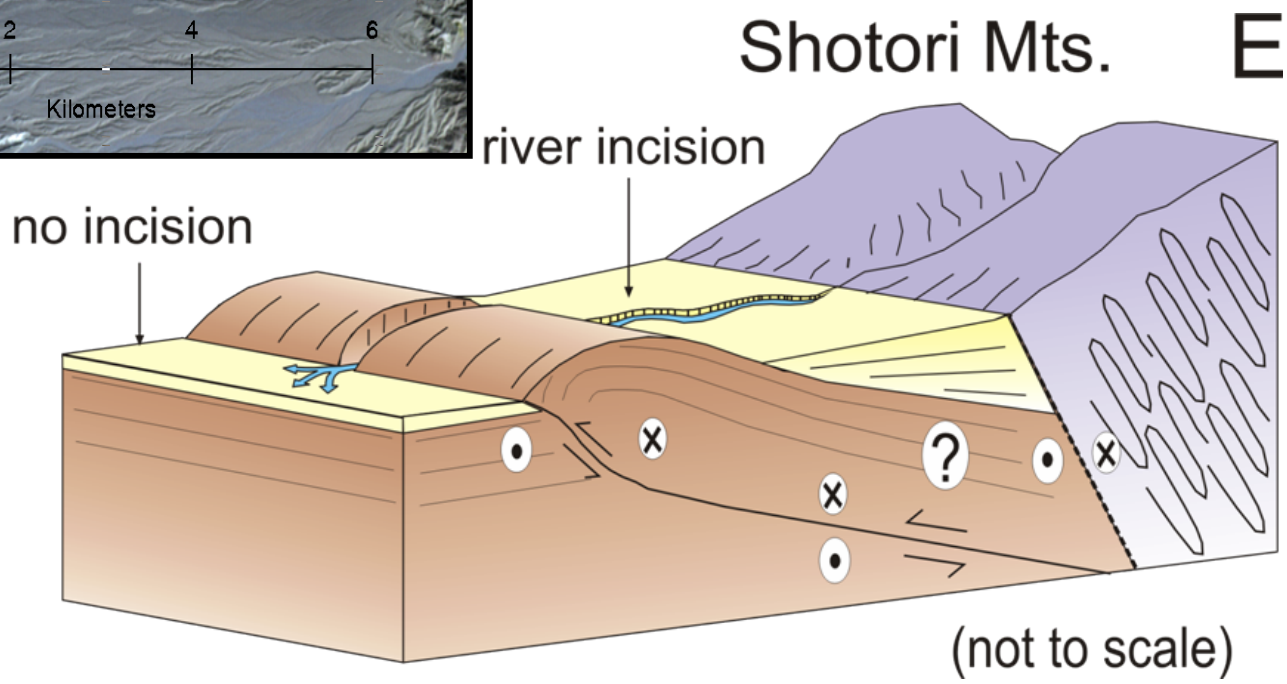
Shotori Mts.
E
river incision
no incision
?
(not to scale)

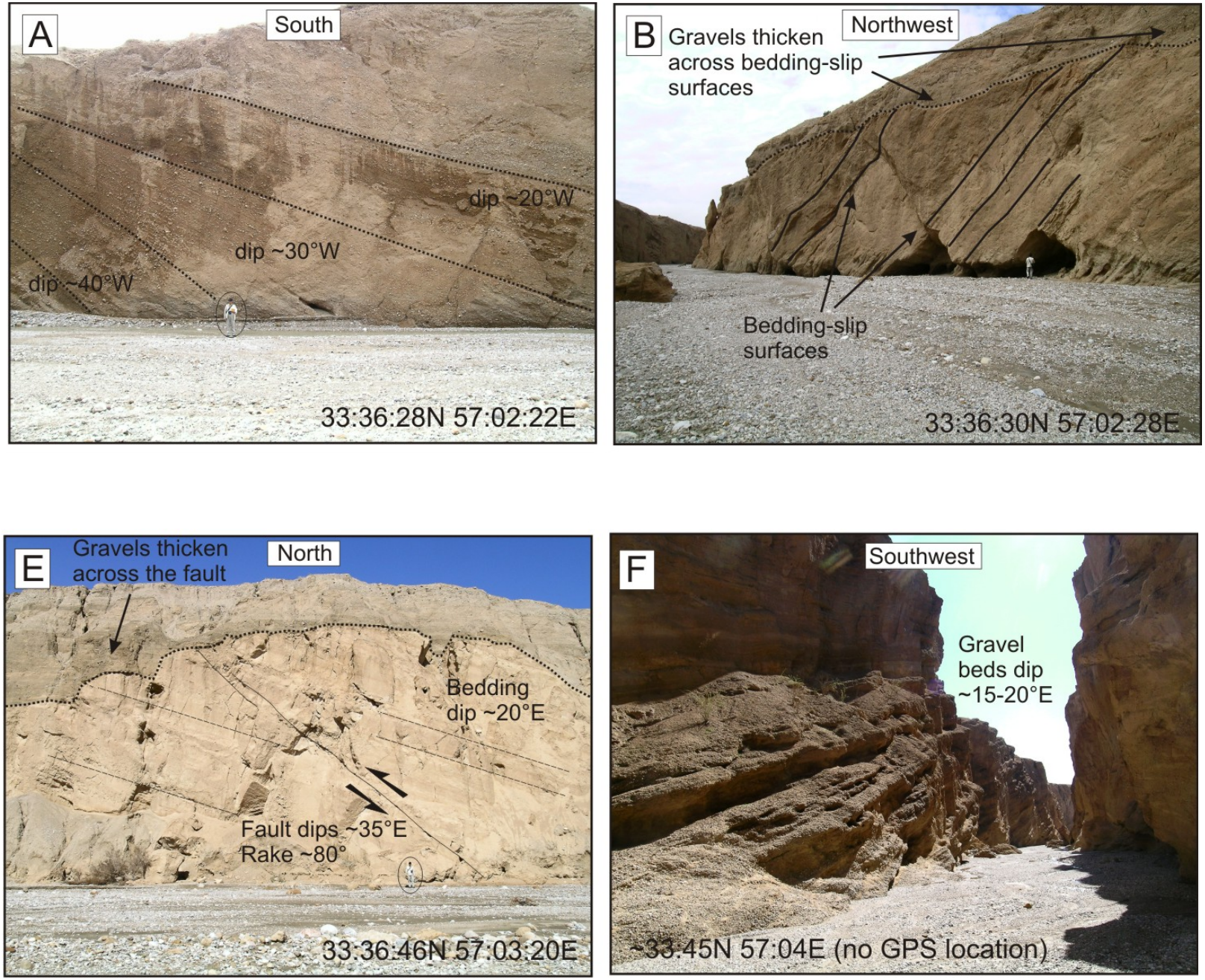
A
South
dip ~20°W
dip ~30°W
dip ~40°W
33:36:28N 57:02:22E
B
Gravels thicken
across bedding-slip
surfaces
Northwest
Bedding-slip
surfaces
33:36:30N 57:02:28E
E
Gravels thicken
across the fault
North
Bedding
dip ~20°E
Fault dips ~35°E
Rake ~80°
33:36:46N 57:03:20E
F
Southwest
Gravel
beds dip
~15-20°E
~33.45N 57:04E (no GPS location)

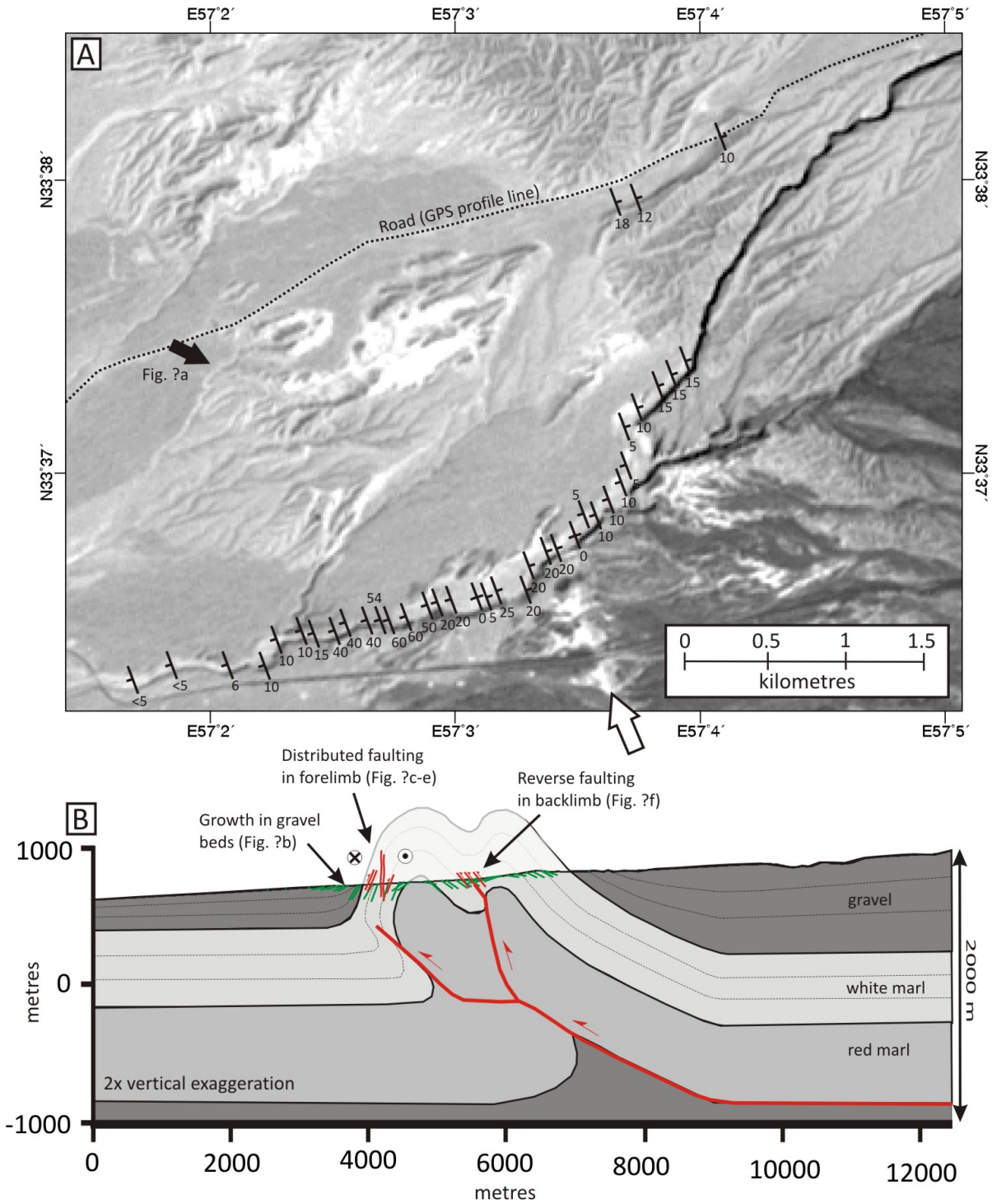
A
E57°2′
E57°3′
E57°4′
E57°5′
N33°38′
N33°37′
Road (GPS profile line)
Fig. ?a
0
0.5
1
1.5
kilometres
B
Distributed faulting
in forelimb (Fig. ?c-e)
Reverse faulting
in backlimb (Fig. ?f)
Growth in gravel
beds (Fig. ?b)
gravel
white marl
red marl
2000 m
2x vertical exaggeration
metres
1000
0
-1000
2000
4000
6000
8000
10000
12000

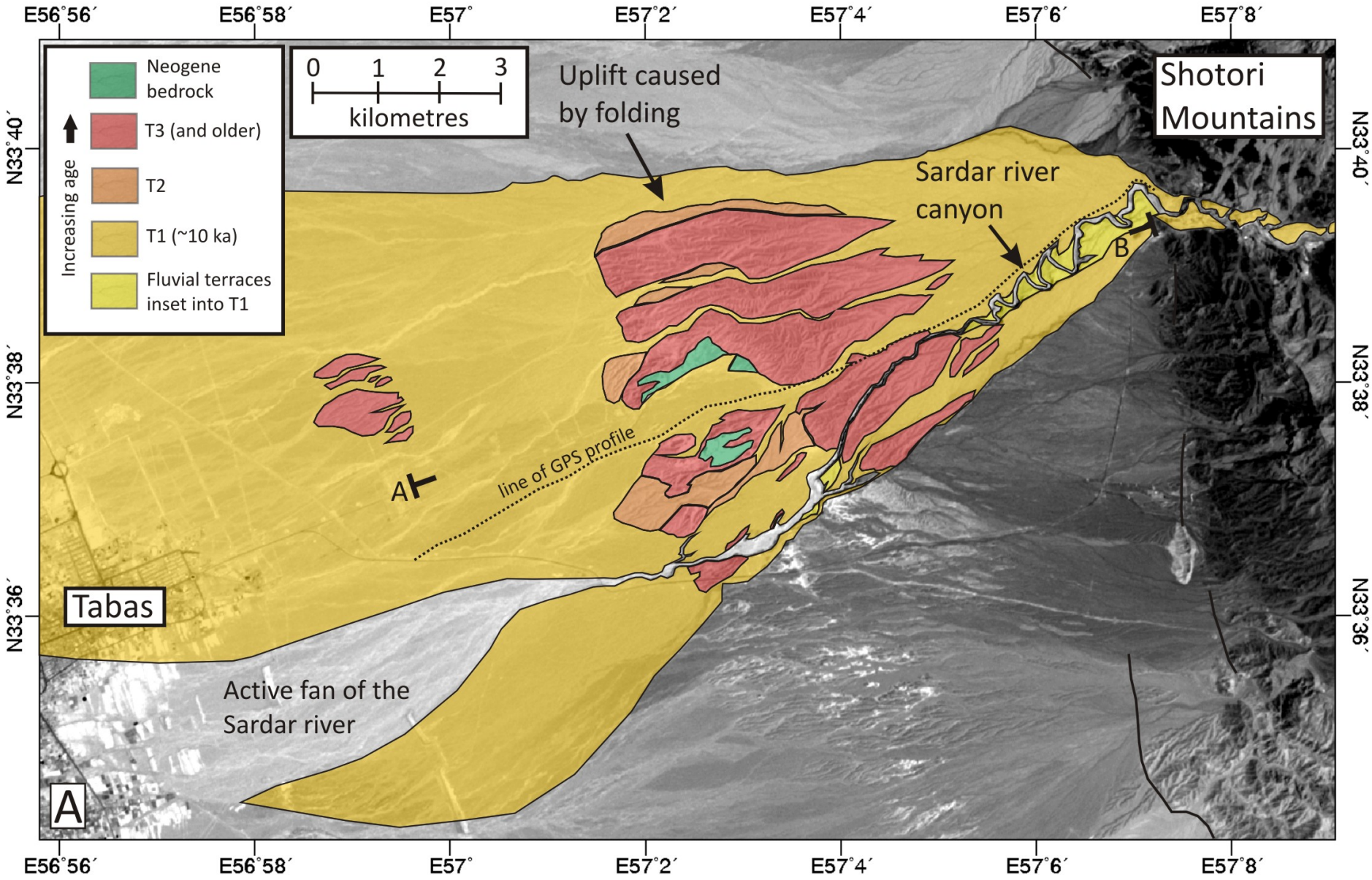
E56°56′
E56°58′
E57°
E57°2′
E57°4′
E57°6′
E57°8′
N33°40′
N33°38′
N33°36′
Neogene bedrock
T3 (and older)
T2
T1 (~10 ka)
Fluvial terraces inset into T1
Increasing age
0 1 2 3
kilometres
Uplift caused by folding
Shotori Mountains
Sardar river canyon
B
A
line of GPS profile
Tabas
Active fan of the Sardar river
A

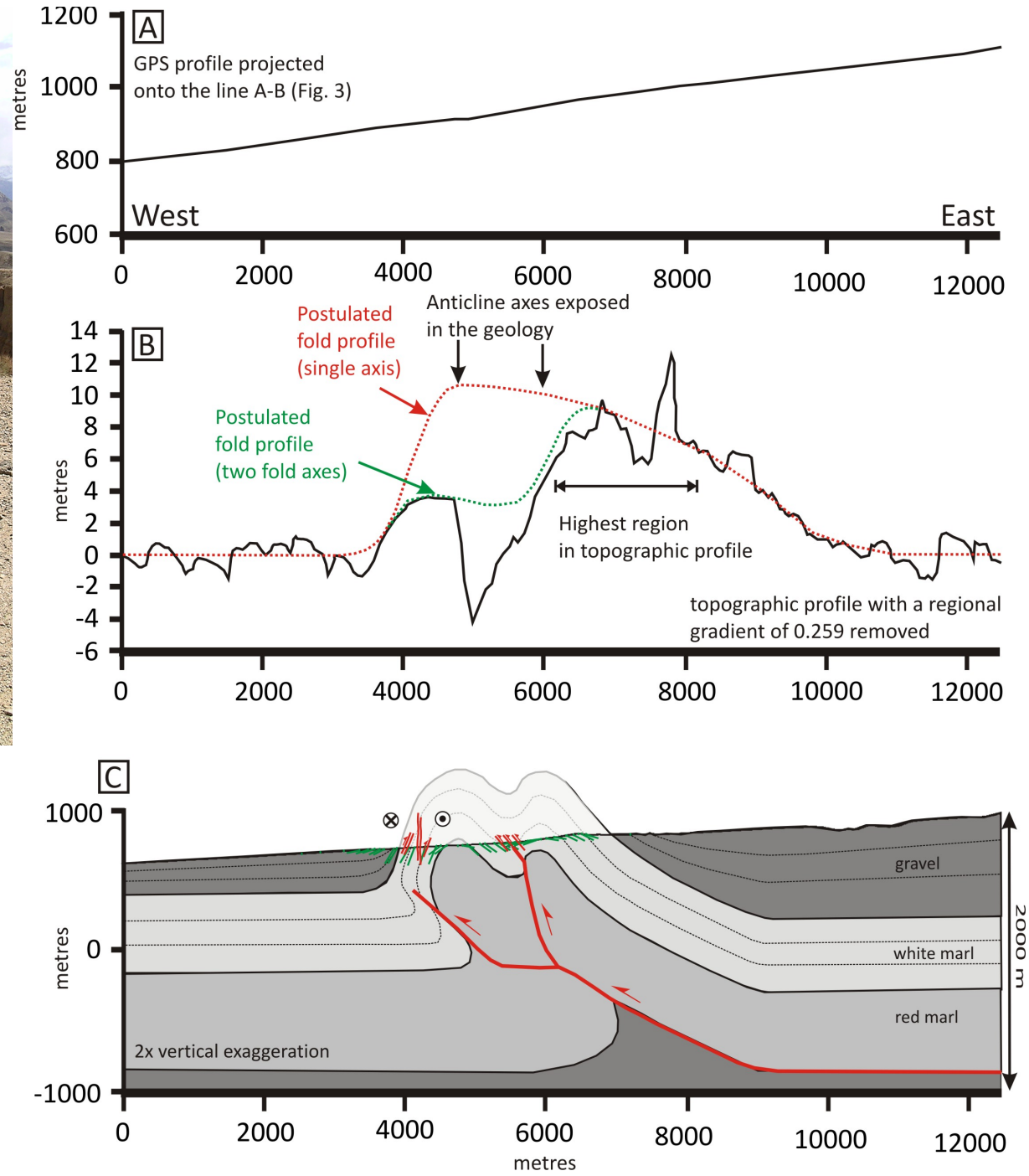
A
GPS profile projected
onto the line A-B (Fig. 3)
metres
1200
1000
800
600
West
East
0
2000
4000
6000
8000
10000
12000
B
Postulated
fold profile
(single axis)
Anticline axes exposed
in the geology
Postulated
fold profile
(two fold axes)
Highest region
in topographic profile
topographic profile with a regional
gradient of 0.259 removed
metres
14
12
10
8
6
4
2
0
-2
-4
-6
C
1000
0
-1000
metres
gravel
white marl
red marl
2000 m
2x vertical exaggeration
0
2000
4000
6000
8000
10000
12000
metres

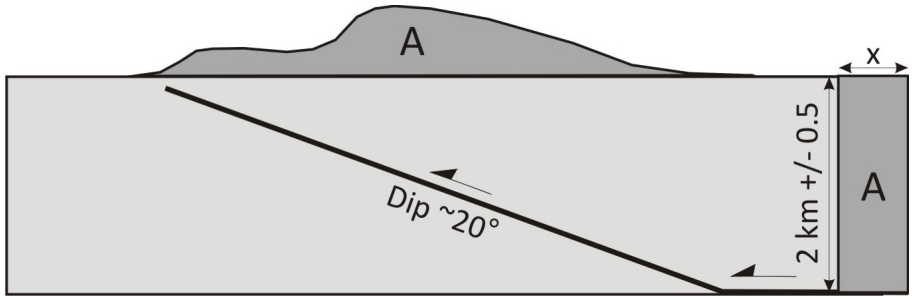
A
x
2 km +/- 0.5
A
Dip ~20°

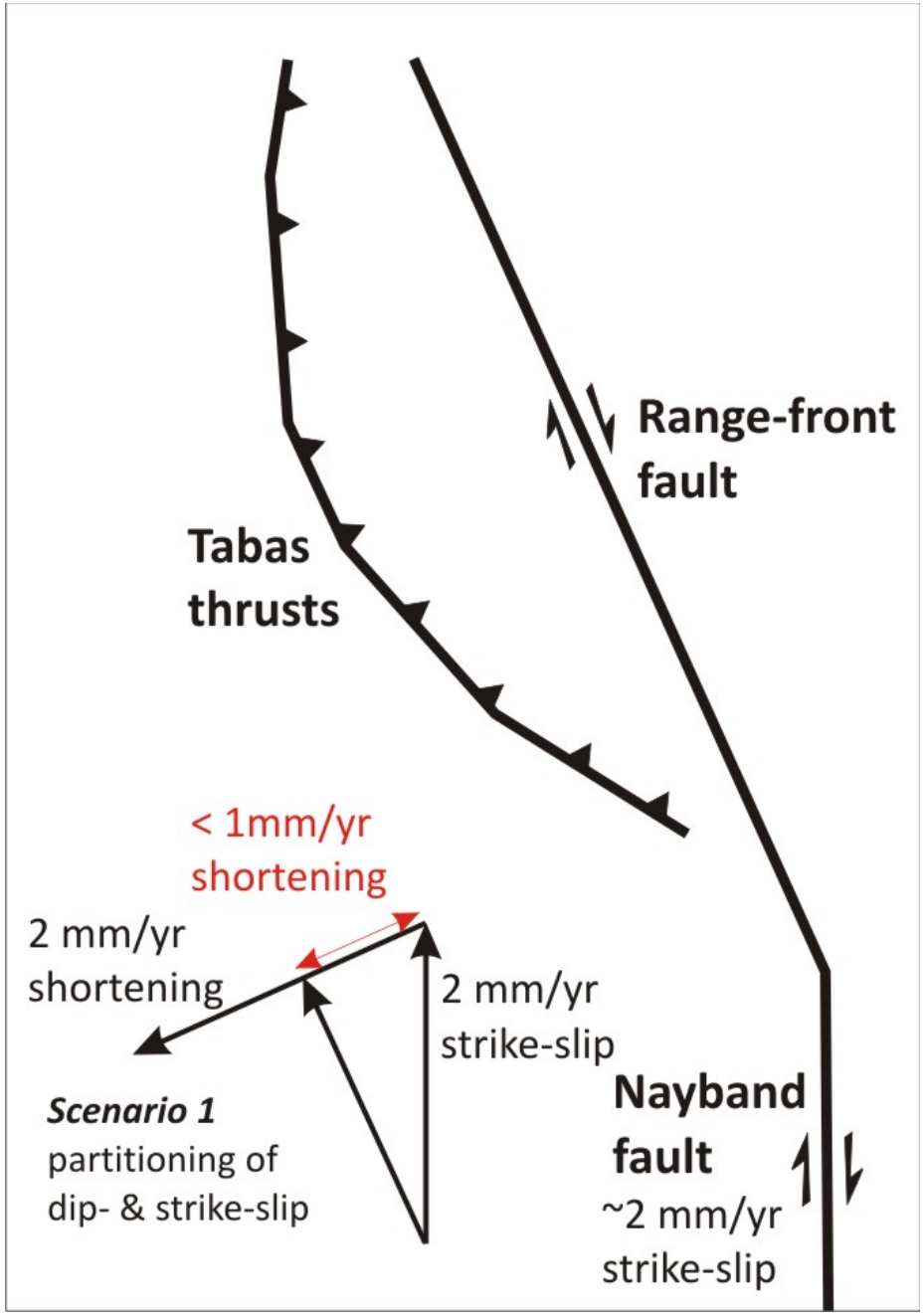
Range-front fault
Tabas thrusts
< 1mm/yr shortening
2 mm/yr shortening
2 mm/yr strike-slip
Scenario 1
partitioning of dip- & strike-slip
Nayband fault
~2 mm/yr strike-slip